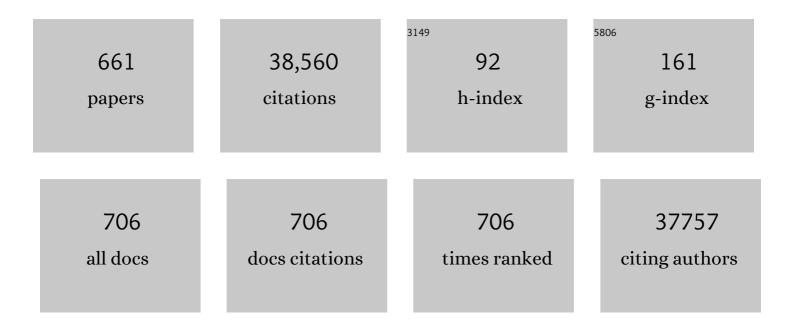
List of Publications by Year in descending order

Source: https://exaly.com/author-pdf/376507/publications.pdf Version: 2024-02-01



SHENC DAI

#	Article	IF	CITATIONS
1	Hydrophobic 1-octadecanethiol functionalized copper catalyst promotes robust high-current CO2 gas-diffusion electrolysis. Nano Research, 2022, 15, 1393-1398.	5.8	19
2	Ultrasound-driven fabrication of high-entropy alloy nanocatalysts promoted by alcoholic ionic liquids. Nano Research, 2022, 15, 4792-4798.	5.8	13
3	Highly Ethylene‧elective Electrocatalytic CO <sub>2</sub> Reduction Enabled by Isolated Cuâ^'S Motifs in Metal–Organic Framework Based Precatalysts. Angewandte Chemie, 2022, 134, .	1.6	5
4	Highly Ethylene‧elective Electrocatalytic CO <sub>2</sub> Reduction Enabled by Isolated Cuâ^'S Motifs in Metal–Organic Framework Based Precatalysts. Angewandte Chemie - International Edition, 2022, 61, .	7.2	81
5	Molecularly Dispersed Cobalt Phthalocyanine Mediates Selective and Durable CO <sub>2</sub> Reduction in a Membrane Flow Cell. Advanced Functional Materials, 2022, 32, 2107301.	7.8	43
6	Graphitic Azaâ€Fused Ï€â€Conjugated Networks: Construction, Engineering, and Taskâ€Specific Applications. Advanced Materials, 2022, 34, e2107947.	11.1	17
7	Selective methane electrosynthesis enabled by a hydrophobic carbon coated copper core–shell architecture. Energy and Environmental Science, 2022, 15, 234-243.	15.6	51
8	Stable Bismuthâ€Doped Lead Halide Perovskite Coreâ€Shell Nanocrystals by Surface Segregation Effect. Small, 2022, 18, e2104399.	5.2	12
9	Newâ€Generation Carbonâ€Capture Ionic Liquids Regulated by Metalâ€ŀon Coordination. ChemSusChem, 2022, 15, .	3.6	8
10	Ligand Defect Density Regulation in Metal–Organic Frameworks by Functional Group Engineering on Linkers. Nano Letters, 2022, 22, 838-845.	4.5	29
11	Beyond Simple Dilution: Superior Conductivities from Cosolvation of Acetonitrile/LiTFSI Concentrated Solution with Acetone. Journal of Physical Chemistry C, 2022, 126, 2788-2796.	1.5	6
12	Induced activation of the commercial Cu/ZnO/Al2O3 catalyst for the steam reforming of methanol. Nature Catalysis, 2022, 5, 99-108.	16.1	155
13	Stable Pd–Cu Hydride Catalyst for Efficient Hydrogen Evolution. Nano Letters, 2022, 22, 1391-1397.	4.5	41
14	Interfacial-confined coordination to single-atom nanotherapeutics. Nature Communications, 2022, 13, 91.	5.8	49
15	Intra-crystalline mesoporous zeolite encapsulation-derived thermally robust metal nanocatalyst in deep oxidation of light alkanes. Nature Communications, 2022, 13, 295.	5.8	54
16	Deep Oxidative Desulfurization of Model Fuels Catalyzed by Subnanosized Ti Oxoclusters. Energy & Fuels, 2022, 36, 1402-1416.	2.5	17
17	Metal–Tannin Coordination Assembly Route to Nanostructured High-Entropy Oxide Perovskites with Abundant Defects. Chemistry of Materials, 2022, 34, 1746-1755.	3.2	14
18	Enhancing Cycling Stability and Capacity Retention of NMC811 Cathodes by Reengineering Interfaces via Electrochemical Fluorination. Advanced Materials Interfaces, 2022, 9, .	1.9	10

#	Article	IF	CITATIONS
19	Dual Rate-Modulation Approach for the Preparation of Crystalline Covalent Triazine Frameworks Displaying Efficient Sodium Storage. ACS Macro Letters, 2022, 11, 60-65.	2.3	12
20	Controlling the elasticity of polyacrylonitrile fibers <i>via</i> ionic liquids containing cyano-based anions. RSC Advances, 2022, 12, 8656-8660.	1.7	2
21	Electrochemical conversion of CO <sub>2</sub> to syngas with a stable H <sub>2</sub> /CO ratio in a wide potential range over ligand-engineered metal–organic frameworks. Journal of Materials Chemistry A, 2022, 10, 9954-9959.	5.2	5
22	Enhanced Hemocompatibility of Silver Nanoparticles Using the Photocatalytic Properties of Titanium Dioxide. Frontiers in Bioengineering and Biotechnology, 2022, 10, 855471.	2.0	2
23	Ionothermal Synthesis of Carbon/TiO <sub>2</sub> Nanocomposite for Supercapacitors. ChemNanoMat, 2022, 8, .	1.5	27
24	Regulating the Spatial Distribution of Ru Nanoparticles on CeO <sub>2</sub> Support for Enhanced Propane Oxidation. ACS Applied Nano Materials, 2022, 5, 3937-3945.	2.4	6
25	Molecularly Dispersed Cobalt Phthalocyanine Mediates Selective and Durable CO <sub>2</sub> Reduction in a Membrane Flow Cell (Adv. Funct. Mater. 11/2022). Advanced Functional Materials, 2022, 32, .	7.8	1
26	Single Atoms Anchored in Hexagonal Boron Nitride for Propane Dehydrogenation from First Principles. ChemCatChem, 2022, 14, .	1.8	6
27	Direct Correlation of the Salt-Reduced Diffusivities of Organic Solvents with the Solvent's Mole Fraction. Journal of Physical Chemistry Letters, 2022, 13, 2845-2850.	2.1	2
28	Mechanochemically Assisted Synthesis of High-Entropy Layer-Structured Dittmarite Analogues. ACS Applied Energy Materials, 2022, 5, 3290-3297.	2.5	8
29	Ultrasound-mediated synthesis of nanoporous fluorite-structured high-entropy oxides toward noble metal stabilization. IScience, 2022, 25, 104214.	1.9	6
30	Reconstructed covalent organic frameworks. Nature, 2022, 604, 72-79.	13.7	190
31	Operando Highâ€Valence Crâ€Modified NiFe Hydroxides for Water Oxidation. Small, 2022, 18, e2200303.	5.2	44
32	In Operando Identification of In Situ Formed Metalloid Zinc <sup>δ+</sup> Active Sites for Highly Efficient Electrocatalyzed Carbon Dioxide Reduction. Angewandte Chemie - International Edition, 2022, 61, .	7.2	25
33	Adding MgCl <sub>2</sub> to Molten NaClâ^UCl <sub><i>n</i></sub> ( <i>n</i> =3, 4): Insights from Firstậ€Principles Molecular Dynamics, ChemPhysChem, 2022, 23 Low-fatigue and large room-temperature elastocaloric effect in a bulk Ti <mml:math< td=""><td>1.0</td><td>2</td></mml:math<>	1.0	2
34	xmlns:mml="http://www.w3.org/1998/Math/MathML" altimg="si16.svg"> <mml:msub><mml:mrow /&gt;<mml:mrow><mml:mn>49.2</mml:mn></mml:mrow></mml:mrow </mml:msub> Ni <mml:math xmlns:mml="http://www.w3.org/1998/Math/MathML" altimg="si17.svg"&gt;<mml:msub></mml:msub></mml:math  > <mml:mrow /&gt;<mml:mrow=>40.8Cu<mml:math< td=""><td>3.8</td><td>17</td></mml:math<></mml:mrow=></mml:mrow 	3.8	17
35	xmlns:mml="http://www.w3.org/1998/Math/MathML" altimg="si18.svg"> <mml:msub><mml:mrow Solm@hotocatalytic Oxidation of Methane to Methanol with Water over RuO<sub><i>x</i></sub>/ZnO/CeO<sub>2</sub> Nanorods. ACS Sustainable Chemistry and Engineering, 2022, 10, 16-22.</mml:mrow </mml:msub>	3.2	30
36	Installation of high-valence tungsten in MIL-125(Ti) for boosted photocatalytic hydrogen evolution. Science China Materials, 2022, 65, 1237-1244.	3.5	4

#	Article	IF	CITATIONS
37	Co-MOF Nanosheets Etched by FeCl <sub>2</sub> Solution for Enhanced Electrocatalytic Oxygen Evolution. Energy & Fuels, 2022, 36, 4524-4531.	2.5	4
38	Waferâ€Scale Demonstration of MBCâ€FET and Câ€FET Arrays Based on Twoâ€Dimensional Semiconductors. Small, 2022, 18, e2107650.	5.2	15
39	Frenkel-defected monolayer MoS2 catalysts for efficient hydrogen evolution. Nature Communications, 2022, 13, 2193.	5.8	137
40	Silicalite-1 Stabilizes Zn-Hydride Species for Efficient Propane Dehydrogenation. ACS Catalysis, 2022, 12, 5997-6006.	5.5	35
41	Design of a multi-functional gel polymer electrolyte with a 3D compact stacked polymer micro-sphere matrix for high-performance lithium metal batteries. Journal of Materials Chemistry A, 2022, 10, 12563-12574.	5.2	31
42	Defect-Regulated Frustrated-Lewis-Pair Behavior of Boron Nitride in Ambient Pressure Hydrogen Activation. Journal of the American Chemical Society, 2022, 144, 10688-10693.	6.6	17
43	Mechanochemistryâ€Driven Construction of Azaâ€fused ï€â€Conjugated Networks Toward Enhanced Energy Storage. Advanced Functional Materials, 2022, 32, .	7.8	9
44	Real-Space Local Dynamics of Molten Inorganic Salts Using Van Hove Correlation Function. Journal of Physical Chemistry Letters, 2022, 13, 5956-5962.	2.1	4
45	Defect Engineering of Ceria Nanocrystals for Enhanced Catalysis via a High-Entropy Oxide Strategy. ACS Central Science, 2022, 8, 1081-1090.	5.3	25
46	Two Ligands of Interest in Recovering Uranium from the Oceans: The Correct Formation Constants of the Uranyl(VI) Cation with 2,2â€2-Bipyridyl-6,6â€2-dicarboxylic Acid and 1,10-Phenanthroline-2,9-dicarboxylic Acid. Inorganic Chemistry, 2022, 61, 9960-9967.	1.9	6
47	Total Oxidation of Light Alkane over Phosphate-Modified Pt/CeO <sub>2</sub> Catalysts. Environmental Science & Technology, 2022, 56, 9661-9671.	4.6	65
48	Enhancing Cycling Stability and Capacity Retention of NMC811 Cathodes by Reengineering Interfaces via Electrochemical Fluorination (Adv. Mater. Interfaces 18/2022). Advanced Materials Interfaces, 2022, 9, .	1.9	1
49	Advanced Transmission Electron Microscopy for Identification of <scp>Atomicâ€Scale</scp> Configurations of <scp>Zeoliteâ€Supported</scp> Metal Catalysts. Chinese Journal of Chemistry, 2022, 40, 2371-2373.	2.6	4
50	Enhanced Oxygen Activation Achieved by Robust Single Chromium Atom-Derived Catalysts in Aerobic Oxidative Desulfurization. ACS Catalysis, 2022, 12, 8623-8631.	5.5	78
51	Sensitive electric field control of first-order phase transition in epitaxial multiferroic heterostructures. Acta Materialia, 2022, 237, 118145.	3.8	1
52	Facilitation of microbially induced calcite precipitation with kaolinite nucleation. Geotechnique, 2021, 71, 728-734.	2.2	15
53	Photo-functionalized TiO2 nanotubes decorated with multifunctional Ag nanoparticles for enhanced vascular biocompatibility. Bioactive Materials, 2021, 6, 45-54.	8.6	25
54	Room temperature synthesis of high-entropy Prussian blue analogues. Nano Energy, 2021, 79, 105464.	8.2	54

#	Article	IF	CITATIONS
55	Modified coal char materials with high rate performance for battery applications. Carbon, 2021, 172, 414-421.	5.4	21
56	Surpassing the Organic Cathode Performance for Lithium-Ion Batteries with Robust Fluorinated Covalent Quinazoline Networks. ACS Energy Letters, 2021, 6, 41-51.	8.8	32
57	Organic wastewater treatment by a single-atom catalyst and electrolytically produced H2O2. Nature Sustainability, 2021, 4, 233-241.	11.5	350
58	Collaboration between a Pt-dimer and neighboring Co–Pd atoms triggers efficient pathways for oxygen reduction reaction. Physical Chemistry Chemical Physics, 2021, 23, 1822-1834.	1.3	16
59	Sacrificial Synthesis of Supported Ru Single Atoms and Clusters on Nâ€doped Carbon Derived from Covalent Triazine Frameworks: A Charge Modulation Approach. Advanced Science, 2021, 8, 2001493.	5.6	38
60	Organic Cathode Materials for Lithiumâ€lon Batteries: Past, Present, and Future. Advanced Energy and Sustainability Research, 2021, 2, 2000044.	2.8	61
61	Sulphur as medium: Directly converting pitch into porous carbon. Fuel, 2021, 286, 119393.	3.4	17
62	Rh nanoparticle functionalized heteroatom-doped hollow carbon spheres for efficient electrocatalytic hydrogen evolution. Materials Chemistry Frontiers, 2021, 5, 3125-3131.	3.2	24
63	Enhanced OER performance of composite Co–Fe-based MOF catalysts <i>via</i> a one-pot ultrasonic-assisted synthetic approach. Sustainable Energy and Fuels, 2021, 5, 1095-1102.	2.5	33
64	A low-valent cobalt oxide co-catalyst to boost photocatalytic water oxidation <i>via</i> enhanced hole-capturing ability. Journal of Materials Chemistry A, 2021, 9, 14786-14792.	5.2	18
65	Interfacial atomic Ni tetragon intercalation in a NiO <sub>2</sub> -to-Pd hetero-structure triggers superior HER activity to the Pt catalyst. Journal of Materials Chemistry A, 2021, 9, 12019-12028.	5.2	19
66	Overcoming the phase separation within high-entropy metal carbide by poly(ionic liquid)s. Chemical Communications, 2021, 57, 3676-3679.	2.2	10
67	Low-Cost Transformation of Biomass-Derived Carbon to High-Performing Nano-graphite via Low-Temperature Electrochemical Graphitization. ACS Applied Materials & Interfaces, 2021, 13, 4393-4401.	4.0	26
68	Bifunctional Pt–SnO <sub>x</sub> nanorods for enhanced oxygen reduction and hydrogen evolution reactions. Sustainable Energy and Fuels, 2021, 5, 2960-2971.	2.5	10
69	Alkaline salt-promoted construction of hydrophilic and nitrogen deficient graphitic carbon nitride with highly improved photocatalytic efficiency. Journal of Materials Chemistry A, 2021, 9, 4700-4706.	5.2	23
70	A template-free synthesis of mesoporous SrTiO <sub>3</sub> single crystals. CrystEngComm, 2021, 23, 5595-5600.	1.3	2
71	Insight into the Solid Electrolyte Interphase Formation in Bis(fluorosulfonyl)Imide Based Ionic Liquid Electrolytes. Advanced Functional Materials, 2021, 31, 2008708.	7.8	30
72	Robust perfluorinated porous organic networks: Succinct synthetic strategy and application in chlorofluorocarbons adsorption. Nano Research, 2021, 14, 3282-3287.	5.8	9

#	Article	IF	CITATIONS
73	Engineering Permanent Porosity into Liquids. Advanced Materials, 2021, 33, e2005745.	11.1	43
74	Perovskite Oxide–Halide Solid Solutions: A Platform for Electrocatalysts. Angewandte Chemie, 2021, 133, 10041-10046.	1.6	3
75	The coefficient of earth pressure at rest in hydrate-bearing sediments. Acta Geotechnica, 2021, 16, 2729-2739.	2.9	14
76	PtAuSn Nanorod Catalysts with a Beneficial Core/Shell Structure for Oxygen Reduction Electrocatalysis. ACS Applied Energy Materials, 2021, 4, 3067-3073.	2.5	8
77	Hierarchical Lignin-Based Carbon Matrix and Carbon Dot Composite Electrodes for High-Performance Supercapacitors. ACS Omega, 2021, 6, 7851-7861.	1.6	20
78	Perovskite Oxide–Halide Solid Solutions: A Platform for Electrocatalysts. Angewandte Chemie - International Edition, 2021, 60, 9953-9958.	7.2	26
79	Strong Enhancement of Nanoconfined Water Mobility by a Structure Breaking Salt. Journal of Physical Chemistry Letters, 2021, 12, 4038-4044.	2.1	7
80	Benzene Ring Knitting Achieved by Ambientâ€Temperature Dehalogenation via Mechanochemical Ullmannâ€Type Reductive Coupling. Advanced Materials, 2021, 33, e2008685.	11.1	27
81	Design of Graphene/Ionic Liquid Composites for Carbon Capture. ACS Applied Materials & Interfaces, 2021, 13, 17511-17516.	4.0	17
82	Molten Salt Assisted Low-Temperature Electro-Catalytic Graphitization of Coal Chars. Journal of the Electrochemical Society, 2021, 168, 046504.	1.3	8
83	Cell-friendly photo-functionalized TiO2 nano-micro-honeycombs for selectively preventing bacteria and platelet adhesion. Materials Science and Engineering C, 2021, 123, 111996.	3.8	4
84	Interactions of an Imine Polymer with Nanoporous Silica and Carbon in Hybrid Adsorbents for Carbon Capture. Langmuir, 2021, 37, 4622-4631.	1.6	7
85	Supramolecular Selfâ€Assembled Multiâ€Electronâ€Acceptor Organic Molecule as Highâ€Performance Cathode Material for Liâ€Ion Batteries. Advanced Energy Materials, 2021, 11, 2100330.	10.2	48
86	High-entropy materials for catalysis: A new frontier. Science Advances, 2021, 7, .	4.7	294
87	Fabrication of Ionic Covalent Triazine Framework-Linked Membranes via a Facile Sol–Gel Approach. Chemistry of Materials, 2021, 33, 3386-3393.	3.2	20
88	Synthesis and Characterization of Macrocyclic Ionic Liquids for CO <sub>2</sub> Separation. Industrial & Engineering Chemistry Research, 2021, 60, 8218-8226.	1.8	6
89	Porous Liquids: Engineering Permanent Porosity into Liquids (Adv. Mater. 18/2021). Advanced Materials, 2021, 33, 2170136.	11.1	3
90	Methane Hydrate Crystallization on Sessile Water Droplets. Journal of Visualized Experiments, 2021, , .	0.2	0

#	Article	IF	CITATIONS
91	Dynamics of Emim <sup>+</sup> in [Emim][TFSI]/LiTFSI Solutions as Bulk and under Confinement in a Quasi-liquid Solid Electrolyte. Journal of Physical Chemistry B, 2021, 125, 5443-5450.	1.2	8
92	Unraveling Local Structure of Molten Salts via X-ray Scattering, Raman Spectroscopy, and <i>Ab Initio</i> Molecular Dynamics. Journal of Physical Chemistry B, 2021, 125, 5971-5982.	1.2	23
93	Role of Organic Fluoride Salts in Stabilizing Niobium Oxo-Clusters Catalyzing Epoxidation. Langmuir, 2021, 37, 8190-8203.	1.6	8
94	CO <sub>2</sub> Chemisorption Behavior of Coordinationâ€Derived Phenolate Sorbents. ChemSusChem, 2021, 14, 2854-2859.	3.6	9
95	Polymer-Grafted Porous Silica Nanoparticles with Enhanced CO <sub>2</sub> Permeability and Mechanical Performance. ACS Applied Materials & Interfaces, 2021, 13, 27411-27418.	4.0	14
96	Formation of three-dimensional bicontinuous structures via molten salt dealloying studied in real-time by in situ synchrotron X-ray nano-tomography. Nature Communications, 2021, 12, 3441.	5.8	36
97	Engineering the Interlayer Spacing by Preâ€Intercalation for High Performance Supercapacitor MXene Electrodes in Room Temperature Ionic Liquid. Advanced Functional Materials, 2021, 31, 2104007.	7.8	64
98	Solid Electrolyte Interphases: Insight into the Solid Electrolyte Interphase Formation in Bis(fluorosulfonyl)Imide Based Ionic Liquid Electrolytes (Adv. Funct. Mater. 23/2021). Advanced Functional Materials, 2021, 31, 2170163.	7.8	0
99	Photoinduced Strong Metal–Support Interaction for Enhanced Catalysis. Journal of the American Chemical Society, 2021, 143, 8521-8526.	6.6	85
100	Molecular Dynamics Simulations of Complexation of Am(III) with a Preorganized Dicationic Ligand in an Ionic Liquid. Journal of Physical Chemistry B, 2021, 125, 8532-8538.	1.2	7
101	Surface enrichment and diffusion enabling gradient-doping and coating of Ni-rich cathode toward Li-ion batteries. Nature Communications, 2021, 12, 4564.	5.8	153
102	Investigating the Degradation of Nb <sub>2</sub> O <sub>5</sub> Thin Films Across 10,000 Lithiation/Delithiation Cycles. ACS Applied Energy Materials, 2021, 4, 6542-6552.	2.5	11
103	Significant Improvement of Catalytic Performance for Chlorinated Volatile Organic Compound Oxidation over RuO <i><sub>x</sub></i> Supported on Acid-Etched Co <sub>3</sub> O <sub>4</sub> . Environmental Science & Technology, 2021, 55, 10734-10743.	4.6	97
104	A Cationic Ru(II) Complex Intercalated into Zirconium Phosphate Layers Catalyzes Selective Hydrogenation via Heterolytic Hydrogen Activation. ChemCatChem, 2021, 13, 3801-3814.	1.8	7
105	CO 2 Chemisorption Behavior of Coordinationâ€Derived Phenolate Sorbents. ChemSusChem, 2021, 14, 2784-2784.	3.6	2
106	Confinement of subnanometric PdCo bimetallic oxide clusters in zeolites for methane complete oxidation. Chemical Engineering Journal, 2021, 418, 129398.	6.6	40
107	Selfâ€Organized Co <sub>3</sub> O <sub>4</sub> ‣rCO <sub>3</sub> Percolative Composites Enabling Nanosized Hole Transport Pathways for Perovskite Solar Cells. Advanced Functional Materials, 2021, 31, 2106121.	7.8	18
108	Formation of LiF Surface Layer During Direct Fluorination of High-Capacity Co-Free Disordered Rocksalt Cathodes. ACS Applied Materials & amp; Interfaces, 2021, 13, 38221-38228.	4.0	13

#	Article	IF	CITATIONS
109	Engineering the Interlayer Spacing by Preâ€Intercalation for High Performance Supercapacitor MXene Electrodes in Room Temperature Ionic Liquid (Adv. Funct. Mater. 33/2021). Advanced Functional Materials, 2021, 31, 2170246.	7.8	2
110	Synthesis of Poly(ionic Liquid)s- <i>block</i> -poly(methyl Methacrylate) Copolymer-Grafted Silica Particle Brushes with Enhanced CO <sub>2</sub> Permeability and Mechanical Performance. Langmuir, 2021, 37, 10875-10881.	1.6	7
111	Exsolution–Dissolution of Supported Metals on High-Entropy Co <sub>3</sub> MnNiCuZnO <i><sub>x</sub></i> : Toward Sintering-Resistant Catalysis. ACS Catalysis, 2021, 11, 12247-12257.	5.5	39
112	Structure–Activity Relationships of Copper- and Potassium-Modified Iron Oxide Catalysts during Reverse Water–Gas Shift Reaction. ACS Catalysis, 2021, 11, 12609-12619.	5.5	48
113	Highly Perfluorinated Covalent Triazine Frameworks Derived from a Lowâ€Temperature Ionothermal Approach Towards Enhanced CO <sub>2</sub> Electroreduction. Angewandte Chemie - International Edition, 2021, 60, 25688-25694.	7.2	36
114	A Holistic Approach for Elucidating Local Structure, Dynamics, and Speciation in Molten Salts with High Structural Disorder. Journal of the American Chemical Society, 2021, 143, 15298-15308.	6.6	20
115	Highly Perfluorinated Covalent Triazine Frameworks Derived fromÂa Lowâ€Temperature IonothermalÂApproach Towards EnhancedÂCO2 Electroreduction. Angewandte Chemie, 2021, 133, 25892.	1.6	2
116	Atomically Dispersed Highâ€Ðensity Al–N <sub>4</sub> Sites in Porous Carbon for Efficient Photodriven CO <sub>2</sub> Cycloaddition. Advanced Materials, 2021, 33, e2103186.	11.1	69
117	Benchmark CO2 separation achieved by highly fluorinated nanoporous molecular sieve membranes from nonporous precursor via in situ cross-linking. Journal of Membrane Science, 2021, 638, 119698.	4.1	6
118	Probing the role of surface hydroxyls for Bi, Sn and In catalysts during CO2 Reduction. Applied Catalysis B: Environmental, 2021, 298, 120581.	10.8	54
119	Towards the object-oriented design of active hydrogen evolution catalysts on single-atom alloys. Chemical Science, 2021, 12, 10634-10642.	3.7	9
120	Radiation-Assisted Formation of Metal Nanoparticles in Molten Salts. Journal of Physical Chemistry Letters, 2021, 12, 157-164.	2.1	14
121	Self-regeneration of supported transition metals by a high entropy-driven principle. Nature Communications, 2021, 12, 5917.	5.8	30
122	Strategies toward the Synthesis of Advanced Functional Sorbent Performance for Uranium Uptake from Seawater. Industrial & Engineering Chemistry Research, 2021, 60, 15037-15044.	1.8	9
123	Flow and Arching of Biomass Particles in Wedge-Shaped Hoppers. ACS Sustainable Chemistry and Engineering, 2021, 9, 15303-15314.	3.2	10
124	Enhanced CO <sub>2</sub> Electrochemical Reduction Performance over Cu@AuCu Catalysts at High Noble Metal Utilization Efficiency. Nano Letters, 2021, 21, 9293-9300.	4.5	33
125	lodine-Doping-Induced Electronic Structure Tuning of Atomic Cobalt for Enhanced Hydrogen Evolution Electrocatalysis. ACS Nano, 2021, 15, 18125-18134.	7.3	40
126	Highly Stretchable, Crack-Insensitive and Compressible Ceramic Aerogel. ACS Nano, 2021, 15, 18354-18362.	7.3	55

#	Article	IF	CITATIONS
127	Operando Analysis of Gas Evolution in TiNb <sub>2</sub> O <sub>7</sub> (TNO)-Based Anodes for Advanced High-Energy Lithium-Ion Batteries under Fast Charging. ACS Applied Materials & Interfaces, 2021, 13, 55145-55155.	4.0	15
128	A high temperature cell for investigating interfacial structure on the molecular scale in molten salt/alloy systems. Review of Scientific Instruments, 2021, 92, 123903.	0.6	1
129	Solvent-free and mechanochemical synthesis of N-doped mesoporous carbon from tannin and related gas sorption property. Chemical Engineering Journal, 2020, 381, 122579.	6.6	39
130	A new trick for an old support: Stabilizing gold single atoms on LaFeO3 perovskite. Applied Catalysis B: Environmental, 2020, 261, 118178.	10.8	31
131	Insights from machine learning of carbon electrodes for electric double layer capacitors. Carbon, 2020, 157, 147-152.	5.4	74
132	Roomâ€Temperature Synthesis of Highâ€Entropy Perovskite Oxide Nanoparticle Catalysts through Ultrasonicationâ€Based Method. ChemSusChem, 2020, 13, 111-115.	3.6	104
133	Lithiophilic V2O5 nanobelt arrays decorated 3D framework hosts for highly stable composite lithium metal anodes. Chemical Engineering Journal, 2020, 384, 123313.	6.6	68
134	Rapid gas-assisted exfoliation promises V2O5 nanosheets for high performance lithium-sulfur batteries. Nano Energy, 2020, 67, 104253.	8.2	106
135	Boosting High-Rate Zinc-Storage Performance by the Rational Design of Mn2O3 Nanoporous Architecture Cathode. Nano-Micro Letters, 2020, 12, 14.	14.4	57
136	Sub-nanometer Pt cluster decoration enhances the oxygen reduction reaction performances of NiO <sub>x</sub> supported Pd nano-islands. Sustainable Energy and Fuels, 2020, 4, 809-823.	2.5	19
137	In situ polymerized succinonitrile-based solid polymer electrolytes for lithium ion batteries. Solid State Ionics, 2020, 345, 115159.	1.3	24
138	O2/N2-responsive microgels as functional draw agents for gas-triggering forward osmosis desalination. Journal of Membrane Science, 2020, 595, 117584.	4.1	7
139	Molecular dynamics simulations of structural and transport properties of molten NaCl-UCl3 using the polarizable-ion model. Journal of Molecular Liquids, 2020, 299, 112184.	2.3	30
140	Uniformity Is Key in Defining Structure–Function Relationships for Atomically Dispersed Metal Catalysts: The Case of Pt/CeO <sub>2</sub> . Journal of the American Chemical Society, 2020, 142, 169-184.	6.6	170
141	Layer-by-Layer Assembly Strategy for Reinforcing the Mechanical Strength of an Ionogel Electrolyte without Affecting Ionic Conductivity. ACS Applied Energy Materials, 2020, 3, 1265-1270.	2.5	12
142	Solvent-free and one-pot synthesis of ultramicroporous carbons with ultrahigh nitrogen contents for sulfur dioxide capture. Chemical Engineering Journal, 2020, 391, 123579.	6.6	32
143	Transforming Porous Organic Cages into Porous Ionic Liquids via a Supramolecular Complexation Strategy. Angewandte Chemie, 2020, 132, 2288-2292.	1.6	21
144	Transforming Porous Organic Cages into Porous Ionic Liquids via a Supramolecular Complexation Strategy. Angewandte Chemie - International Edition, 2020, 59, 2268-2272.	7.2	101

#	Article	IF	CITATIONS
145	Addition of Chloroform in a Solvent-in-Salt Electrolyte: Outcomes in the Microscopic Dynamics in Bulk and Confinement. Journal of Physical Chemistry C, 2020, 124, 22366-22375.	1.5	7
146	Broadening the Gas Separation Utility of Monolayer Nanoporous Graphene Membranes by an Ionic Liquid Gating. Nano Letters, 2020, 20, 7995-8000.	4.5	39
147	Hierarchically Porous Polyacrylonitrile (PAN) 3D Architectures with Anchored Lattice-Expanded λ-MnO <sub>2</sub> Nanodots as Freestanding Adsorbents for Superior Lithium Separation. Industrial & Engineering Chemistry Research, 2020, 59, 13239-13245.	1.8	9
148	Tuning the Cation–Anion Interactions by Methylation of the Pyridinium Cation: An X-ray Photoelectron Spectroscopy Study of Picolinium Ionic Liquids. Journal of Physical Chemistry B, 2020, 124, 6657-6663.	1.2	8
149	Direct Transformation of Glycerol to Propanal using Zirconium Phosphateâ€Supported Bimetallic Catalysts. ChemSusChem, 2020, 13, 4954-4966.	3.6	15
150	Deep Understanding of Strong Metal Interface Confinement: A Journey of Pd/FeO <sub><i>x</i></sub> Catalysts. ACS Catalysis, 2020, 10, 8950-8959.	5.5	113
151	Sizeâ€Dependent Nickelâ€Based Electrocatalysts for Selective CO <sub>2</sub> Reduction. Angewandte Chemie - International Edition, 2020, 59, 18572-18577.	7.2	100
152	Sizeâ€Dependent Nickelâ€Based Electrocatalysts for Selective CO <sub>2</sub> Reduction. Angewandte Chemie, 2020, 132, 18731-18736.	1.6	30
153	Self-regenerative noble metal catalysts supported on high-entropy oxides. Chemical Communications, 2020, 56, 15056-15059.	2.2	34
154	Porous Liquids: The Next Frontier. CheM, 2020, 6, 3263-3287.	5.8	57
155	Alcohol-Induced Low-Temperature Blockage of Supported-Metal Catalysts for Enhanced Catalysis. ACS Catalysis, 2020, 10, 8515-8523.	5.5	18
156	Electrode material–ionic liquid coupling for electrochemical energy storage. Nature Reviews Materials, 2020, 5, 787-808.	23.3	210
157	Tuning regioselective oxidation toward phenol via atomically dispersed iron sites on carbon. Green Chemistry, 2020, 22, 6025-6032.	4.6	9
158	In Situ TEM Studies of Catalysts Using Windowed Gas Cells. Catalysts, 2020, 10, 779.	1.6	21
159	What Fluorine Can Do in CO <sub>2</sub> Chemistry: Applications from Homogeneous to Heterogeneous Systems. ChemSusChem, 2020, 13, 6182-6200.	3.6	18
160	Entropy-stabilized single-atom Pd catalysts via high-entropy fluorite oxide supports. Nature Communications, 2020, 11, 3908.	5.8	172
161	Mechanochemical Synthesis of High-Purity Anhydrous Binary Alkali and Alkaline Earth Chloride Mixtures. Industrial & Engineering Chemistry Research, 2020, 59, 19884-19889.	1.8	3
	Mainly on the Plane: Deep Subsurface Bacterial Proteins Bind and Alter Clathrate Structure. Crystal		

#	Article	IF	CITATIONS
163	MEMS-based dual temperature control measurement method for thermoelectric properties of individual nanowires. MRS Communications, 2020, 10, 620-627.	0.8	3
164	H <sub>2</sub> O-prompted CO <sub>2</sub> capture on metal silicates <i>in situ</i> generated from SBA-15. RSC Advances, 2020, 10, 28731-28740.	1.7	3
165	Ambient Temperature Graphitization Based on Mechanochemical Synthesis. Angewandte Chemie, 2020, 132, 22119-22123.	1.6	3
166	Ambient Temperature Graphitization Based on Mechanochemical Synthesis. Angewandte Chemie - International Edition, 2020, 59, 21935-21939.	7.2	32
167	Sinter-Resistant Nanoparticle Catalysts Achieved by 2D Boron Nitride-Based Strong Metal–Support Interactions: A New Twist on an Old Story. ACS Central Science, 2020, 6, 1617-1627.	5.3	42
168	Thermoregulated Ionic Liquid-Stabilizing Ru/CoO Nanocomposites for Catalytic Hydrogenation. Langmuir, 2020, 36, 11589-11599.	1.6	12
169	Structure and dynamics of the molten alkali-chloride salts from an X-ray, simulation, and rate theory perspective. Physical Chemistry Chemical Physics, 2020, 22, 22900-22917.	1.3	22
170	Directly Probing Local Coordination, Charge State and Stability of Single Atom Catalysts. Microscopy and Microanalysis, 2020, 26, 2468-2469.	0.2	1
171	Roles of niobium in the dehydrogenation of propane to propylene over a Pt/Nb-modified Al <sub>2</sub> O <sub>3</sub> catalyst. New Journal of Chemistry, 2020, 44, 20115-20121.	1.4	3
172	A Principle for Highly Active Metal Oxide Catalysts via NaCl-Based Solid Solution. CheM, 2020, 6, 1723-1741.	5.8	30
173	Encapsulated Sb and Sb <sub>2</sub> O <sub>3</sub> particles in waste-tire derived carbon as stable composite anodes for sodium-ion batteries. Sustainable Energy and Fuels, 2020, 4, 3613-3622.	2.5	13
174	Sodium Oxide Cathodes: Insights into the Enhanced Cycle and Rate Performances of the Fâ€6ubstituted P2â€Type Oxide Cathodes for Sodiumâ€Ion Batteries (Adv. Energy Mater. 19/2020). Advanced Energy Materials, 2020, 10, 2070087.	10.2	2
175	X-ray photoelectron spectroscopy of piperidinium ionic liquids: a comparison to the charge delocalised pyridinium analogues. Physical Chemistry Chemical Physics, 2020, 22, 11976-11983.	1.3	7
176	Carbon Coated Porous Titanium Niobium Oxides as Anode Materials of Lithium-Ion Batteries for Extreme Fast Charge Applications. ACS Applied Energy Materials, 2020, 3, 5657-5665.	2.5	53
177	Holey Lamellar Highâ€Entropy Oxide as an Ultraâ€Highâ€Activity Heterogeneous Catalyst for Solventâ€free Aerobic Oxidation of Benzyl Alcohol. Angewandte Chemie - International Edition, 2020, 59, 19503-19509.	7.2	157
178	Synthesizing High apacity Oxyfluoride Conversion Anodes by Direct Fluorination of Molybdenum Dioxide (MoO <sub>2</sub> ). ChemSusChem, 2020, 13, 3825-3834.	3.6	12
179	Prediction by Convolutional Neural Networks of CO <sub>2</sub> /N <sub>2</sub> Selectivity in Porous Carbons from N <sub>2</sub> Adsorption Isotherm at 77 K. Angewandte Chemie, 2020, 132, 19813-19816.	1.6	7
180	Harnessing strong metal–support interactions via a reverse route. Nature Communications, 2020, 11, 3042.	5.8	84

#	Article	IF	CITATIONS
181	Direct Recycling of Spent NCM Cathodes through Ionothermal Lithiation. Advanced Energy Materials, 2020, 10, 2001204.	10.2	129
182	Prediction by Convolutional Neural Networks of CO <sub>2</sub> /N <sub>2</sub> Selectivity in Porous Carbons from N <sub>2</sub> Adsorption Isotherm at 77 K. Angewandte Chemie - International Edition, 2020, 59, 19645-19648.	7.2	26
183	Highly efficient alloyed NiCu/Nb <sub>2</sub> O <sub>5</sub> catalyst for the hydrodeoxygenation of biofuel precursors into liquid alkanes. Catalysis Science and Technology, 2020, 10, 4256-4263.	2.1	22
184	Synthesis of Ionic Ultramicroporous Polymers for Selective Separation of Acetylene from Ethylene. Advanced Materials, 2020, 32, e1907601.	11.1	54
185	Ionic Liquidâ€Directed Nanoporous TiNb <sub>2</sub> O <sub>7</sub> Anodes with Superior Performance for Fastâ€Rechargeable Lithiumâ€Ion Batteries. Small, 2020, 16, e2001884.	5.2	69
186	Local synergetic collaboration between Pd and local tetrahedral symmetric Ni oxide enables ultra-high-performance CO <sub>2</sub> thermal methanation. Journal of Materials Chemistry A, 2020, 8, 12744-12756.	5.2	18
187	Incorporating Lanthanum into Mesoporous Silica Foam Enhances Enzyme Immobilization and the Activity of Penicillin G Acylase Due to Lewis Acidâ€Base Interactions. ChemBioChem, 2020, 21, 2143-2148.	1.3	4
188	Temperature Dependence of Short and Intermediate Range Order in Molten MgCl <sub>2</sub> and Its Mixture with KCl. Journal of Physical Chemistry B, 2020, 124, 2892-2899.	1.2	38
189	Boosting electrosynthesis of ammonia on surface-engineered MXene Ti3C2. Nano Energy, 2020, 72, 104681.	8.2	82
190	Optimization of Pt–Oxygen-Containing Species Anodes for Ethanol Oxidation Reaction: High Performance of Pt-AuSnO <sub><i>x</i></sub> Electrocatalyst. Journal of Physical Chemistry Letters, 2020, 11, 2846-2853.	2.1	11
191	Photofunctionalized and Drug-Loaded TiO <sub>2</sub> Nanotubes with Improved Vascular Biocompatibility as a Potential Material for Polymer-Free Drug-Eluting Stents. ACS Biomaterials Science and Engineering, 2020, 6, 2038-2049.	2.6	12
192	Transformation Strategy for Highly Crystalline Covalent Triazine Frameworks: From Staggered AB to Eclipsed AA Stacking. Journal of the American Chemical Society, 2020, 142, 6856-6860.	6.6	136
193	Ion-gated carbon molecular sieve gas separation membranes. Journal of Membrane Science, 2020, 604, 118013.	4.1	15
194	Revealing 3D Morphological and Chemical Evolution Mechanisms of Metals in Molten Salt by Multimodal Microscopy. ACS Applied Materials & Interfaces, 2020, 12, 17321-17333.	4.0	20
195	Insights into the Enhanced Cycle and Rate Performances of the Fâ€6ubstituted P2â€Type Oxide Cathodes for Sodiumâ€Ion Batteries. Advanced Energy Materials, 2020, 10, 2000135.	10.2	57
196	Solventâ€Free Selfâ€Assembly for Scalable Preparation of Highly Crystalline Mesoporous Metal Oxides. Angewandte Chemie - International Edition, 2020, 59, 11053-11060.	7.2	68
197	Tailoring Polymer Colloids Derived Porous Carbon Spheres Based on Specific Chemical Reactions. Advanced Materials, 2020, 32, e2002475.	11.1	69
198	Connections between the Speciation and Solubility of Ni(II) and Co(II) in Molten ZnCl <sub>2</sub> . Journal of Physical Chemistry B, 2020, 124, 1253-1258.	1.2	24

#	Article	IF	CITATIONS
199	Anisotropic and hierarchical SiC@SiO <sub>2</sub> nanowire aerogel with exceptional stiffness and stability for thermal superinsulation. Science Advances, 2020, 6, eaay6689.	4.7	164
200	Facile synthesis of a linear porous organic polymer <i>via</i> Schiff-base chemistry for propyne/propylene separation. Polymer Chemistry, 2020, 11, 4382-4386.	1.9	8
201	Across the Board: Sheng Dai on Catalyst Design by Entropic Factors. ChemSusChem, 2020, 13, 1915-1917.	3.6	17
202	High-Entropy Perovskite Fluorides: A New Platform for Oxygen Evolution Catalysis. Journal of the American Chemical Society, 2020, 142, 4550-4554.	6.6	208
203	Mechanochemical synthesis of pillar[5]quinone derived multi-microporous organic polymers for radioactive organic iodide capture and storage. Nature Communications, 2020, 11, 1086.	5.8	87
204	Interfacial Biocatalytic Performance of Nanofiber-Supported β-Galactosidase for Production of Galacto-Oligosaccharides. Catalysts, 2020, 10, 81.	1.6	7
205	<i>De novo</i> fabrication of multi-heteroatom-doped carbonaceous materials <i>via</i> an <i>in situ</i> doping strategy. Journal of Materials Chemistry A, 2020, 8, 4740-4746.	5.2	11
206	Effect of the Ionic Liquid Structure on the Melt Processability of Polyacrylonitrile Fibers. ACS Applied Materials & Interfaces, 2020, 12, 8663-8673.	4.0	9
207	Surpassing Robeson Upper Limit for CO2/N2 Separation with Fluorinated Carbon Molecular Sieve Membranes. CheM, 2020, 6, 631-645.	5.8	73
208	Electrochemically induced crystallization of amorphous materials in molten MgCl <sub>2</sub> : boron nitride and hard carbon. Chemical Communications, 2020, 56, 2783-2786.	2.2	10
209	Thermal and magnetic dual-responsive l-proline nanohybrids for aqueous asymmetric aldol reaction. Reactive and Functional Polymers, 2020, 149, 104508.	2.0	8
210	Kinetic Isotope Effect as a Tool To Investigate the Oxygen Reduction Reaction on Ptâ€based Electrocatalysts – Part II: Effect of Platinum Dispersion. ChemPhysChem, 2020, 21, 1331-1339.	1.0	4
211	Synergistic effect of dual BrÃ,nsted acidic deep eutectic solvents for oxidative desulfurization of diesel fuel. Chemical Engineering Journal, 2020, 394, 124831.	6.6	123
212	Pore‣cale Controls on the Gas and Water Transport in Hydrateâ€Bearing Sediments. Geophysical Research Letters, 2020, 47, e2020GL086990.	1.5	17
213	An ultrastable heterostructured oxide catalyst based on high-entropy materials: A new strategy toward catalyst stabilization via synergistic interfacial interaction. Applied Catalysis B: Environmental, 2020, 276, 119155.	10.8	72
214	Two-in-one: construction of hydroxyl and imidazolium-bifunctionalized ionic networks in one-pot toward synergistic catalytic CO <sub>2</sub> fixation. Chemical Communications, 2020, 56, 3309-3312.	2.2	92
215	Facile benzene reduction promoted by a synergistically coupled Cu–Co–Ce ternary mixed oxide. Chemical Science, 2020, 11, 5766-5771.	3.7	8
216	Uniphase ruthenium–iridium alloy-based electronic regulation for electronic structure–function study in methane oxidation to methanol. Journal of Materials Chemistry A, 2020, 8, 24024-24030.	5.2	15

#	Article	IF	CITATIONS
217	(Physical and Analytical Electrochemistry Division Max Bredig Award Address In Molten Salt and Ionic) Tj ETQq1 Transactions, 2020, 98, 3-8.	1 0.784314 0.3	ł rgBT /Over 0
218	Nahinfrarotaktive Bleichalkogenidâ€Quantenpunkte: Herstellung, postsynthetischer Ligandenaustausch und Anwendungen in Solarzellen. Angewandte Chemie, 2019, 131, 5256-5279.	1.6	4
219	Nearâ€Infrared Active Lead Chalcogenide Quantum Dots: Preparation, Postâ€Synthesis Ligand Exchange, and Applications in Solar Cells. Angewandte Chemie - International Edition, 2019, 58, 5202-5224.	7.2	86
220	Solvothermal and template-free synthesis of N-Functionalized mesoporous polymer for amine impregnation and CO2 adsorption. Microporous and Mesoporous Materials, 2019, 290, 109653.	2.2	28
221	Transmission Electron Microscopy of Catalytic Nanomaterials at Atomic Resolution. Microscopy and Microanalysis, 2019, 25, 2054-2055.	0.2	0
222	Enabling chloride salts for thermal energy storage: implications of salt purity. RSC Advances, 2019, 9, 25602-25608.	1.7	55
223	Topotactic Synthesis of Phosphabenzeneâ€Functionalized Porous Organic Polymers: Efficient Ligands in CO 2 Conversion. Angewandte Chemie, 2019, 131, 13901-13905.	1.6	3
224	Topotactic Synthesis of Phosphabenzeneâ€Functionalized Porous Organic Polymers: Efficient Ligands in CO <sub>2</sub> Conversion. Angewandte Chemie - International Edition, 2019, 58, 13763-13767.	7.2	32
225	Investigating the Nature of the Active Sites for the CO <sub>2</sub> Reduction Reaction on Carbon-Based Electrocatalysts. ACS Catalysis, 2019, 9, 7668-7678.	5.5	58
226	A dicyanobenzoquinone based cathode material for rechargeable lithium and sodium ion batteries. Journal of Materials Chemistry A, 2019, 7, 17888-17895.	5.2	35
227	Simultaneous activation and N-doping of hydrothermal carbons by NaNH2: An effective approach to CO2 adsorbents. Journal of CO2 Utilization, 2019, 33, 405-412.	3.3	19
228	Entropic selectivity in air separation <i>via</i> a bilayer nanoporous graphene membrane. Physical Chemistry Chemical Physics, 2019, 21, 16310-16315.	1.3	3
229	Mechanochemical Nonhydrolytic Sol–Gel-Strategy for the Production of Mesoporous Multimetallic Oxides. Chemistry of Materials, 2019, 31, 5529-5536.	3.2	65
230	Influence of fluorination on CO <sub>2</sub> adsorption in materials derived from fluorinated covalent triazine framework precursors. Journal of Materials Chemistry A, 2019, 7, 17277-17282.	5.2	47
231	Insights into CO <sub>2</sub> /N <sub>2</sub> Selectivity in Porous Carbons from Deep Learning. , 2019, 1, 558-563.		34
232	From Highly Purified Boron Nitride to Boron Nitrideâ€Based Heterostructures: An Inorganic Precursorâ€Based Strategy. Advanced Functional Materials, 2019, 29, 1906284.	7.8	22
233	Simultaneously Boosting the Ionic Conductivity and Mechanical Strength of Polymer Gel Electrolyte Membranes by Confining Ionic Liquids into Hollow Silica Nanocavities. Batteries and Supercaps, 2019, 2, 985-991.	2.4	21
234	Bioelectrochemical Reaction Kinetics, Mechanisms, and Pathways of Chlorophenol Degradation in MFC Using Different Microbial Consortia. ACS Sustainable Chemistry and Engineering, 2019, 7, 17263-17272.	3.2	27

#	Article	IF	CITATIONS
235	Tuning Electronic Structure and Lattice Diffusion Barrier of Ternary Pt–In–Ni for Both Improved Activity and Stability Properties in Oxygen Reduction Electrocatalysis. ACS Catalysis, 2019, 9, 11431-11437.	5.5	36
236	Design and Synthesis of Highly-Dispersed WO <sub>3</sub> Catalyst with Highly Effective NH <sub>3</sub> –SCR Activity for NO <sub><i>x</i></sub> Abatement. ACS Catalysis, 2019, 9, 11557-11562.	5.5	50
237	<i>In situ</i> Cathodoluminescence and Monitoring Electronic Structure Change Using Optical TEM Holder. Microscopy and Microanalysis, 2019, 25, 2302-2303.	0.2	1
238	Developing Multifunctional and High Resolution In-situ TEM Holders. Microscopy and Microanalysis, 2019, 25, 1854-1855.	0.2	0
239	Unexpected Strong Thermally Induced Phonon Energy Shift for Mapping Local Temperature. Nano Letters, 2019, 19, 7494-7502.	4.5	17
240	Porous liquid zeolites: hydrogen bonding-stabilized H-ZSM-5 in branched ionic liquids. Nanoscale, 2019, 11, 1515-1519.	2.8	82
241	Decoupling the roles of carbon and metal oxides on the electrocatalytic reduction of oxygen on La <sub>1â^'x</sub> Sr <sub>x</sub> CoO <sub>3â^îſ</sub> perovskite composite electrodes. Physical Chemistry Chemical Physics, 2019, 21, 3327-3338.	1.3	26
242	Platinum-trimer decorated cobalt-palladium core-shell nanocatalyst with promising performance for oxygen reduction reaction. Nature Communications, 2019, 10, 440.	5.8	115
243	A Polymerâ€Oriented Selfâ€Assembly Strategy toward Mesoporous Metal Oxides with Ultrahigh Surface Areas. Advanced Science, 2019, 6, 1801543.	5.6	25
244	Solventâ€Induced Selfâ€Assembly Strategy to Synthesize Wellâ€Defined Hierarchically Porous Polymers. Advanced Materials, 2019, 31, e1806254.	11.1	79
245	Probing microstructure and electrolyte concentration dependent cell chemistry <i>via operando</i> small angle neutron scattering. Energy and Environmental Science, 2019, 12, 1866-1877.	15.6	36
246	Heterogeneous viologen catalysts for metal-free and selective oxidations. Green Chemistry, 2019, 21, 1455-1460.	4.6	31
247	Mechanochemical synthesis of metal–organic frameworks. Polyhedron, 2019, 162, 59-64.	1.0	161
248	Achieving an exceptionally high loading of isolated cobalt single atoms on a porous carbon matrix for efficient visible-light-driven photocatalytic hydrogen production. Chemical Science, 2019, 10, 2585-2591.	3.7	50
249	In situ Scanning Transmission Electron Microscopy with Atomic Resolution under Atmospheric Pressure. Microscopy Today, 2019, 27, 16-21.	0.2	1
250	Mechanochemical Synthesis of High Entropy Oxide Materials under Ambient Conditions: Dispersion of Catalysts via Entropy Maximization. , 2019, 1, 83-88.		143
251	Perfect Andreev reflection due to the Klein paradox in a topological superconducting state. Nature, 2019, 570, 344-348.	13.7	38
252	Catalysts in Coronas: A Surface Spatial Confinement Strategy for High-Performance Catalysts in Methane Dry Reforming. ACS Catalysis, 2019, 9, 9072-9080.	5.5	121

#	Article	IF	CITATIONS
253	Promoting Pt catalysis for CO oxidation <i>via</i> the Mott–Schottky effect. Nanoscale, 2019, 11, 18568-18574.	2.8	13
254	Construction of a Nanoporous Highly Crystalline Hexagonal Boron Nitride from an Amorphous Precursor for Catalytic Dehydrogenation. Angewandte Chemie - International Edition, 2019, 58, 10626-10630.	7.2	55
255	N-cyclic quaternary ammonium-functionalized anion exchange membrane with improved alkaline stability enabled by aryl-ether free polymer backbones for alkaline fuel cells. Journal of Membrane Science, 2019, 587, 117135.	4.1	53
256	Active and stable Pt-Ceria nanowires@silica shell catalyst: Design, formation mechanism and total oxidation of CO and toluene. Applied Catalysis B: Environmental, 2019, 256, 117807.	10.8	57
257	Construction of a Nanoporous Highly Crystalline Hexagonal Boron Nitride from an Amorphous Precursor for Catalytic Dehydrogenation. Angewandte Chemie, 2019, 131, 10736-10740.	1.6	7
258	Boric acid-based ternary deep eutectic solvent for extraction and oxidative desulfurization of diesel fuel. Green Chemistry, 2019, 21, 3074-3080.	4.6	151
259	Single-atom tailoring of platinum nanocatalysts for high-performance multifunctional electrocatalysis. Nature Catalysis, 2019, 2, 495-503.	16.1	464
260	Defectâ€Tailoring Mediated Electron–Hole Separation in Singleâ€Unitâ€Cell Bi <sub>3</sub> O <sub>4</sub> Br Nanosheets for Boosting Photocatalytic Hydrogen Evolution and Nitrogen Fixation. Advanced Materials, 2019, 31, e1807576.	11.1	311
261	Structural evolution of atomically dispersed Pt catalysts dictates reactivity. Nature Materials, 2019, 18, 746-751.	13.3	404
262	Mechanochemical Synthesis of Ruthenium Cluster@Ordered Mesoporous Carbon Catalysts by Synergetic Dual Templates. Chemistry - A European Journal, 2019, 25, 8494-8498.	1.7	10
263	Fewâ€Layer Boron Nitride with Engineered Nitrogen Vacancies for Promoting Conversion of Polysulfide as a Cathode Matrix for Lithium–Sulfur Batteries. Chemistry - A European Journal, 2019, 25, 8112-8117.	1.7	39
264	Microporous and hollow carbon spheres derived from soft drinks: Promising CO2 separation materials. Microporous and Mesoporous Materials, 2019, 286, 199-206.	2.2	15
265	Spaceâ€Confined Polymerization: Controlled Fabrication of Nitrogenâ€Doped Polymer and Carbon Microspheres with Refined Hierarchical Architectures. Advanced Materials, 2019, 31, e1807876.	11.1	127
266	Entropyâ€Maximized Synthesis of Multimetallic Nanoparticle Catalysts via a Ultrasonicationâ€Assisted Wet Chemistry Method under Ambient Conditions. Advanced Materials Interfaces, 2019, 6, 1900015.	1.9	130
267	High-performance electrolytic oxygen evolution with a seamless armor core–shell FeCoNi oxynitride. Nanoscale, 2019, 11, 7239-7246.	2.8	28
268	Facile Synthesis of Copper Containing Ordered Mesoporous Polymers via Aqueous Coordination Self-Assembly for Aerobic Oxidation of Alcohols. Industrial & Engineering Chemistry Research, 2019, 58, 6438-6445.	1.8	9
269	Taming the stability of Pd active phases through a compartmentalizing strategy toward nanostructured catalyst supports. Nature Communications, 2019, 10, 1611.	5.8	168
270	Hysteretic order-disorder transitions of ionic liquid double layer structure on graphite. Nano Energy, 2019, 60, 886-893.	8.2	19

#	Article	IF	CITATIONS
271	Heterogeneity of polyoxometalates by confining within ordered mesopores: toward efficient oxidation of benzene to phenol. Catalysis Science and Technology, 2019, 9, 2173-2179.	2.1	12
272	Fluorination of MXene by Elemental F 2 as Electrode Material for Lithiumâ€ion Batteries. ChemSusChem, 2019, 12, 1271-1271.	3.6	0
273	Tetrahydrofuran Hydrate in Clayey Sediments—Laboratory Formation, Morphology, and Wave Characterization. Journal of Geophysical Research: Solid Earth, 2019, 124, 3307-3319.	1.4	56
274	Chemical Approaches to Carbonâ€Based Metalâ€Free Catalysts. Advanced Materials, 2019, 31, e1804863.	11.1	90
275	Cation Molecular Structure Affects Mobility and Transport of Electrolytes in Porous Carbons. Journal of the Electrochemical Society, 2019, 166, A507-A514.	1.3	12
276	Entropyâ€Driven Mechanochemical Synthesis of Polymetallic Zeolitic Imidazolate Frameworks for CO <sub>2</sub> Fixation. Angewandte Chemie, 2019, 131, 5072-5076.	1.6	27
277	Entropyâ€Driven Mechanochemical Synthesis of Polymetallic Zeolitic Imidazolate Frameworks for CO <sub>2</sub> Fixation. Angewandte Chemie - International Edition, 2019, 58, 5018-5022.	7.2	107
278	Siderophore-inspired chelator hijacks uranium from aqueous medium. Nature Communications, 2019, 10, 819.	5.8	84
279	First-Principles Molecular Dynamics Simulations of UCl <sub><i>n</i></sub> –NaCl ( <i>n</i> = 3, 4) Molten Salts. ACS Applied Energy Materials, 2019, 2, 2122-2128.	2.5	39
280	Fluorination of MXene by Elemental F <sub>2</sub> as Electrode Material for Lithiumâ€ion Batteries. ChemSusChem, 2019, 12, 1316-1324.	3.6	28
281	Oxidation-Induced Atom Diffusion and Surface Restructuring in Faceted Ternary Pt–Cu–Ni Nanoparticles. Chemistry of Materials, 2019, 31, 1720-1728.	3.2	30
282	Mineral Weathering and Bedrock Weakening: Modeling Microscale Bedrock Damage Under Biotite Weathering. Journal of Geophysical Research F: Earth Surface, 2019, 124, 2623-2646.	1.0	14
283	A succinct strategy for construction of nanoporous ionic organic networks from a pyrylium intermediate. Chemical Communications, 2019, 55, 13450-13453.	2.2	9
284	Aluminum hydroxide-mediated synthesis of mesoporous metal oxides by a mechanochemical nanocasting strategy. Journal of Materials Chemistry A, 2019, 7, 22977-22985.	5.2	20
285	Polyoxometalates as bifunctional templates: engineering metal oxides with mesopores and reactive surfaces for catalysis. Journal of Materials Chemistry A, 2019, 7, 27297-27303.	5.2	9
286	Elucidating Ionic Correlations Beyond Simple Charge Alternation in Molten MgCl <sub>2</sub> –KCl Mixtures. Journal of Physical Chemistry Letters, 2019, 10, 7603-7610.	2.1	49
287	A pore-scale numerical investigation of the effect of pore characteristics on flow properties in soils. Journal of Zhejiang University: Science A, 2019, 20, 961-978.	1.3	5
288	Effects of water on the stochastic motions of propane confined in MCM-41-S pores. Physical Chemistry Chemical Physics, 2019, 21, 25035-25046.	1.3	16

#	Article	IF	CITATIONS
289	Coupling FeNi alloys and hollow nitrogen-enriched carbon frameworks leads to high-performance oxygen electrocatalysts for rechargeable zinc–air batteries. Sustainable Energy and Fuels, 2019, 3, 136-141.	2.5	34
290	Continuously Tunable Pore Size for Gas Separation via a Bilayer Nanoporous Graphene Membrane. ACS Applied Nano Materials, 2019, 2, 379-384.	2.4	34
291	Non-ionic copolymer microgels as high-performance draw materials for forward osmosis desalination. Journal of Membrane Science, 2019, 572, 480-488.	4.1	29
292	Enhanced Cycling Performance for Lithium–Sulfur Batteries by a Laminated 2D g <sub>3</sub> N <sub>4</sub> /Graphene Cathode Interlayer. ChemSusChem, 2019, 12, 213-223.	3.6	72
293	Ionic Gating of Ultrathin and Leaky Ferroelectrics. Advanced Materials Interfaces, 2019, 6, 1801723.	1.9	8
294	Complexation of lanthanides and other metal ions by the polypyridyl ligand quaterpyridine: Relation between metal ion size, chelate ring size, and complex stability. Inorganica Chimica Acta, 2019, 488, 19-27.	1.2	10
295	Characterization and Engineering Properties of Dry and Ponded Class-F Fly Ash. Journal of Geotechnical and Geoenvironmental Engineering - ASCE, 2019, 145, .	1.5	25
296	Optimizing the structural configuration of FePt-FeOx nanoparticles at the atomic scale by tuning the post-synthetic conditions. Nano Energy, 2019, 55, 441-446.	8.2	10
297	Deep eutectic solvents formed by quaternary ammonium salts and aprotic organic compound succinonitrile. Journal of Molecular Liquids, 2019, 274, 414-417.	2.3	23
298	Reply to the Correspondence on "Preorganization and Cooperation for Highly Efficient and Reversible Capture of Low oncentration CO <sub>2</sub> by Ionic Liquids― Angewandte Chemie - International Edition, 2019, 58, 386-389.	7.2	17
299	Confined Ionic Liquid in an Ionic Porous Aromatic Framework for Gas Separation. ACS Applied Polymer Materials, 2019, 1, 95-102.	2.0	20
300	Confinement of Ultrasmall Cobalt Oxide Clusters within Silicalite-1 Crystals for Efficient Conversion of Fructose into Methyl Lactate. ACS Catalysis, 2019, 9, 1923-1930.	5.5	39
301	Prediction of Carbon Dioxide Adsorption via Deep Learning. Angewandte Chemie, 2019, 131, 265-269.	1.6	45
302	Prediction of Carbon Dioxide Adsorption via Deep Learning. Angewandte Chemie - International Edition, 2019, 58, 259-263.	7.2	74
303	Bis(trimethylsilyl) 2-fluoromalonate derivatives as electrolyte additives for high voltage lithium ion batteries. Journal of Power Sources, 2019, 412, 527-535.	4.0	47
304	Understanding the effect of molecular solvents on the microscopic network of DBU imidazole ionic liquid. Journal of Molecular Liquids, 2019, 276, 325-333.	2.3	10
305	Developed one-pot synthesis of dual-color CdSe quantum dots for white light-emitting diode application. Journal of Materials Chemistry C, 2018, 6, 3089-3096.	2.7	16
306	Preparation of a mesocellular siliceous foam supported lanthanide-sensitive polymer for the selective adsorption of lanthanides. Dalton Transactions, 2018, 47, 4840-4846.	1.6	4

#	Article	IF	CITATIONS
307	A chelation-induced cooperative self-assembly methodology for the synthesis of mesoporous metal hydroxide and oxide nanospheres. Nanoscale, 2018, 10, 5731-5737.	2.8	21
308	Polydopamineâ€Ðerived, In Situ Nâ€Ðoped 3D Mesoporous Carbons for Highly Efficient Oxygen Reduction. ChemNanoMat, 2018, 4, 417-422.	1.5	19
309	Enhanced multi-lineage differentiation of human mesenchymal stem/stromal cells within poly( <i>N</i> -isopropylacrylamide-acrylic acid) microgel-formed three-dimensional constructs. Journal of Materials Chemistry B, 2018, 6, 1799-1814.	2.9	16
310	Multistage Triaxial Tests on Laboratoryâ€Formed Methane Hydrateâ€Bearing Sediments. Journal of Geophysical Research: Solid Earth, 2018, 123, 3347-3357.	1.4	77
311	Mechanochemicalâ€Assisted Synthesis of Highâ€Entropy Metal Nitride via a Soft Urea Strategy. Advanced Materials, 2018, 30, e1707512.	11.1	325
312	Ultraâ€Stable and Highâ€Cobaltâ€Loaded Cobalt@Ordered Mesoporous Carbon Catalysts: Allâ€inâ€One Deoxygenation of Ketone into Alkylbenzene. ChemCatChem, 2018, 10, 3299-3304.	1.8	17
313	Synthesis of Porous Sulfonamide Polymers by Capturing Atmospheric Sulfur Dioxide. ChemSusChem, 2018, 11, 1751-1755.	3.6	11
314	Gas-responsive cationic microgels for forward osmosis desalination. Chemical Engineering Journal, 2018, 347, 424-431.	6.6	28
315	Engineering nanoporous organic frameworks to stabilize naked Au clusters: a charge modulation approach. Chemical Communications, 2018, 54, 5058-5061.	2.2	19
316	Improved Lubricating Performance by Combining Oil-Soluble Hairy Silica Nanoparticles and an Ionic Liquid as an Additive for a Synthetic Base Oil. ACS Applied Materials & Interfaces, 2018, 10, 15129-15139.	4.0	51
317	Effects of amine loading on the properties of cellulose nanofibrils aerogel and its CO2 capturing performance. Carbohydrate Polymers, 2018, 194, 252-259.	5.1	63
318	Facile Synthesis of Highly Porous Metal Oxides by Mechanochemical Nanocasting. Chemistry of Materials, 2018, 30, 2924-2929.	3.2	54
319	Fibers with Hyperâ€Crosslinked Functional Porous Frameworks. Macromolecular Rapid Communications, 2018, 39, 1700767.	2.0	8
320	Interface Engineering of Earth-Abundant Transition Metals Using Boron Nitride for Selective Electroreduction of CO <sub>2</sub> . ACS Applied Materials & Interfaces, 2018, 10, 6694-6700.	4.0	52
321	Ionic liquids and derived materials for lithium and sodium batteries. Chemical Society Reviews, 2018, 47, 2020-2064.	18.7	452
322	Electrocatalytic Activity of a 2D Phosphoreneâ€Based Heteroelectrocatalyst for Photoelectrochemical Cells. Angewandte Chemie - International Edition, 2018, 57, 2644-2647.	7.2	48
323	Aromatic Polyimide/Graphene Composite Organic Cathodes for Fast and Sustainable Lithiumâ€ion Batteries. ChemSusChem, 2018, 11, 763-772.	3.6	58
324	New Class of Type III Porous Liquids: A Promising Platform for Rational Adjustment of Gas Sorption Behavior. ACS Applied Materials & Interfaces, 2018, 10, 32-36.	4.0	142

#	Article	IF	CITATIONS
325	Accelerating Membraneâ€based CO <sub>2</sub> Separation by Soluble Nanoporous Polymer Networks Produced by Mechanochemical Oxidative Coupling. Angewandte Chemie - International Edition, 2018, 57, 2816-2821.	7.2	44
326	Accelerating Membraneâ€based CO <sub>2</sub> Separation by Soluble Nanoporous Polymer Networks Produced by Mechanochemical Oxidative Coupling. Angewandte Chemie, 2018, 130, 2866-2871.	1.6	10
327	Smart Pd Catalyst with Improved Thermal Stability Supported on High-Surface-Area LaFeO <sub>3</sub> Prepared by Atomic Layer Deposition. Journal of the American Chemical Society, 2018, 140, 4841-4848.	6.6	85
328	SO <sub>2</sub> absorption in EmimCl–TEG deep eutectic solvents. Physical Chemistry Chemical Physics, 2018, 20, 15168-15173.	1.3	76
329	Controlling the magic size of white light-emitting CdSe quantum dots. Nanoscale, 2018, 10, 10256-10261.	2.8	10
330	Structure and Dynamics of Polymeric Canopies in Nanoscale Ionic Materials: An Electrical Double Layer Perspective. Scientific Reports, 2018, 8, 5191.	1.6	6
331	Sproutâ€like Growth of Mesoporous Mo <sub>2</sub> C/NC Nanonetworks as Efficient Electrocatalysts for Hydrogen Evolution. ChemCatChem, 2018, 10, 625-631.	1.8	15
332	Microbial community and bioelectrochemical activities in MFC for degrading phenol and producing electricity: Microbial consortia could make differences. Chemical Engineering Journal, 2018, 332, 647-657.	6.6	137
333	Hydrophobic Solid Acids and Their Catalytic Applications in Green and Sustainable Chemistry. ACS Catalysis, 2018, 8, 372-391.	5.5	200
334	Interfacial Engineering of Supported Liquid Membranes by Vapor Crossâ€Linking for Enhanced Separation of Carbon Dioxide. ChemSusChem, 2018, 11, 185-192.	3.6	7
335	Double-tilt in situ TEM Holder with Ultra-high Stability. Microscopy and Microanalysis, 2018, 24, 1890-1891.	0.2	0
336	Extraction of Rare Earths in Ionic Liquids <i>Via</i> Competitive Ligand Complexation between TODGA and DTPA. Solvent Extraction and Ion Exchange, 2018, 36, 574-582.	0.8	6
337	A benzoquinone-derived porous hydrophenazine framework for efficient and reversible iodine capture. Chemical Communications, 2018, 54, 12706-12709.	2.2	28
338	Controlled synthesis of hierarchical ZSM-5 for catalytic fast pyrolysis of cellulose to aromatics. Journal of Materials Chemistry A, 2018, 6, 21178-21185.	5.2	38
339	Investigating Thermal Behavior of Surface Phonon in SiC by in-situ Vibrational Spectroscopy. Microscopy and Microanalysis, 2018, 24, 416-417.	0.2	0
340	Understanding Electric Double-Layer Gating Based on Ionic Liquids: from Nanoscale to Macroscale. ACS Applied Materials & Interfaces, 2018, 10, 43211-43218.	4.0	21
341	Cold Cluster–CeO <sub>2</sub> Nanostructured Hybrid Architectures as Catalysts for Selective Oxidation of Inert Hydrocarbons. Chemistry of Materials, 2018, 30, 8579-8586.	3.2	16
342	In situ Scanning Transmission Electron Microscopy with Atomic Resolution under Atmospheric Pressures. Microscopy and Microanalysis, 2018, 24, 234-235.	0.2	1

#	Article	IF	CITATIONS
343	Integrated Surface Functionalization of Li-Rich Cathode Materials for Li-Ion Batteries. ACS Applied Materials & Interfaces, 2018, 10, 41802-41813.	4.0	56
344	Pyrolyzed Triazine-Based Nanoporous Frameworks Enable Electrochemical CO <sub>2</sub> Reduction in Water. ACS Applied Materials & Interfaces, 2018, 10, 43588-43594.	4.0	29
345	Reply to the Correspondence on "Preorganization and Cooperation for Highly Efficient and Reversible Capture of Low oncentration CO 2 by Ionic Liquids― Angewandte Chemie, 2018, 131, 392.	1.6	0
346	Open and Hierarchical Carbon Framework with Ultralarge Pore Volume for Efficient Capture of Carbon Dioxide. ACS Applied Materials & amp; Interfaces, 2018, 10, 36961-36968.	4.0	59
347	Trimethyl phosphate based neutral ligand room temperature ionic liquids for electrodeposition of rare earth elements. Electrochemistry Communications, 2018, 96, 88-92.	2.3	27
348	Promotion of Ternary Pt–Sn–Ag Catalysts toward Ethanol Oxidation Reaction: Revealing Electronic and Structural Effects of Additive Metals. ACS Energy Letters, 2018, 3, 2550-2557.	8.8	41
349	Deconvolution of octahedral Pt3Ni nanoparticle growth pathway from in situ characterizations. Nature Communications, 2018, 9, 4485.	5.8	37
350	NIPAM-based Microgel Microenvironment Regulates the Therapeutic Function of Cardiac Stromal Cells. ACS Applied Materials & amp; Interfaces, 2018, 10, 37783-37796.	4.0	32
351	Tuning microenvironment for multicellular spheroid formation in thermoâ€responsive anionic microgel scaffolds. Journal of Biomedical Materials Research - Part A, 2018, 106, 2899-2909.	2.1	10
352	Synergistic Effect of F <sup>–</sup> Doping and LiF Coating on Improving the High-Voltage Cycling Stability and Rate Capacity of LiNi <sub>0.5</sub> Co <sub>0.2</sub> Mn <sub>0.3</sub> O <sub>2</sub> Cathode Materials for Lithium-Ion Batteries. ACS Applied Materials & Interfaces, 2018, 10, 34153-34162.	4.0	129
353	Electrophoretic Deposition of Mesoporous Niobium(V)Oxide Nanoscopic Films. Chemistry of Materials, 2018, 30, 6549-6558.	3.2	16
354	Confined Ultrathin Pd e Nanowires with Outstanding Moisture and SO <sub>2</sub> Tolerance in Methane Combustion. Angewandte Chemie - International Edition, 2018, 57, 8953-8957.	7.2	124
355	Confined Ultrathin Pdâ€Ce Nanowires with Outstanding Moisture and SO 2 Tolerance in Methane Combustion. Angewandte Chemie, 2018, 130, 9091-9095.	1.6	25
356	Comparative microscopic dynamics in a room-temperature ionic liquid confined in carbon pores characterized by reversible and irreversible ion immobilization. AIP Conference Proceedings, 2018, , .	0.3	3
357	In situ Atmospheric Transmission Electron Microscopy of Catalytic Nanomaterials. MRS Advances, 2018, 3, 2297-2303.	0.5	2
358	Carbon/tin oxide composite electrodes for improved lithium-ion batteries. Journal of Applied Electrochemistry, 2018, 48, 811-817.	1.5	13
359	Synergistic Enhancement in Antibacterial Activity of Core/Shell/Shell SiO <sub>2</sub> /ZnO/Ag <sub>3</sub> PO <sub>4</sub> Nanoparticles. ChemNanoMat, 2018, 4, 972-981.	1.5	10
360	Combining <i>In-Situ</i> Transmission Electron Microscopy and Infrared Spectroscopy for Understanding Dynamic and Atomic-Scale Features of Supported Metal Catalysts. Journal of Physical Chemistry C, 2018, 122, 25143-25157.	1.5	41

#	Article	IF	CITATIONS
361	All-solid-state interpenetrating network polymer electrolytes for long cycle life of lithium metal batteries. Journal of Materials Chemistry A, 2018, 6, 14847-14855.	5.2	44
362	Mesoporous Carbon Nanospheres as a Multifunctional Carrier for Cancer Theranostics. Theranostics, 2018, 8, 663-675.	4.6	99
363	Methyl quantum tunneling in ionic liquid [DMIm][TFSI] facilitated by Bis(trifluoromethane)sulfonimide lithium salt. Scientific Reports, 2018, 8, 10354.	1.6	5
364	Effects of Confinement and Pressure on the Vibrational Behavior of Nano-Confined Propane. Journal of Physical Chemistry A, 2018, 122, 6736-6745.	1.1	20
365	Defect Engineering in Polymeric Cobalt Phthalocyanine Networks for Enhanced Electrochemical CO <sub>2</sub> Reduction. ChemElectroChem, 2018, 5, 2717-2721.	1.7	52
366	Effect of pore density on gas permeation through nanoporous graphene membranes. Nanoscale, 2018, 10, 14660-14666.	2.8	31
367	Tailoring the Selectivity of Bioâ€Ethanol Transformation by Tuning the Size of Gold Supported on ZnZr <sub>10</sub> O <sub>x</sub> Catalysts. ChemCatChem, 2018, 10, 3969-3973.	1.8	8
368	Double-tilt in situ TEM holder with ultra-high stability. Ultramicroscopy, 2018, 192, 1-6.	0.8	8
369	In Situ TEM Probing of Ferroelectric Switching under Electrical Bias. Microscopy and Microanalysis, 2018, 24, 1812-1813.	0.2	1
370	Supported bicyclic amidine ionic liquids as a potential CO2/N2 separation medium. Journal of Membrane Science, 2018, 565, 203-212.	4.1	24
371	Synergistic Activation of Palladium Nanoparticles by Polyoxometalateâ€Attached Melem for Boosting Formic Acid Dehydrogenation Efficiency. ChemSusChem, 2018, 11, 3396-3401.	3.6	23
372	Synthesis of Porous Polymeric Catalysts for the Conversion of Carbon Dioxide. ACS Catalysis, 2018, 8, 9079-9102.	5.5	196
373	Ion Dynamics in Ionicâ€Liquidâ€Based Liâ€Ion Electrolytes Investigated by Neutron Scattering and Dielectric Spectroscopy. ChemSusChem, 2018, 11, 3512-3523.	3.6	22
374	Coordination-supported organic polymers: mesoporous inorganic–organic materials with preferred stability. Inorganic Chemistry Frontiers, 2018, 5, 2018-2022.	3.0	5
375	Entropy-stabilized metal oxide solid solutions as CO oxidation catalysts with high-temperature stability. Journal of Materials Chemistry A, 2018, 6, 11129-11133.	5.2	196
376	Tuning the Core–Shell Structure of Au144@Fe2O3 for Optimal Catalytic Activity for CO Oxidation. Catalysis Letters, 2018, 148, 2315-2324.	1.4	3
377	Reversible Control of Interfacial Magnetism through Ionic-Liquid-Assisted Polarization Switching. Nano Letters, 2017, 17, 1665-1669.	4.5	28
378	Pyrolysis of conjugated nanoporous polycarbazoles to mesoporous N-doped carbon nanotubes as efficient electrocatalysts for the oxygen reduction reaction. Journal of Materials Chemistry A, 2017, 5, 4507-4512.	5.2	41

#	Article	IF	CITATIONS
379	Electrochemically Driven Transformation of Amorphous Carbons to Crystalline Graphite Nanoflakes: A Facile and Mild Graphitization Method. Angewandte Chemie - International Edition, 2017, 56, 1751-1755.	7.2	83
380	Electrochemically Driven Transformation of Amorphous Carbons to Crystalline Graphite Nanoflakes: A Facile and Mild Graphitization Method. Angewandte Chemie, 2017, 129, 1777-1781.	1.6	56
381	<i>In Situ</i> Observation of Rh-CaTiO <sub>3</sub> Catalysts during Reduction and Oxidation Treatments by Transmission Electron Microscopy. ACS Catalysis, 2017, 7, 1579-1582.	5.5	51
382	Aminopolymer functionalization of boron nitride nanosheets for highly efficient capture of carbon dioxide. Journal of Materials Chemistry A, 2017, 5, 16241-16248.	5.2	67
383	Ion-Gated Gas Separation through Porous Graphene. Nano Letters, 2017, 17, 1802-1807.	4.5	109
384	High-surface-area, iron-oxide films prepared by atomic layer deposition on γ-Al2O3. Applied Catalysis A: General, 2017, 534, 70-77.	2.2	34
385	Selective separation of americium from europium using 2,9-bis(triazine)-1,10-phenanthrolines in ionic liquids: a new twist on an old story. Chemical Communications, 2017, 53, 2744-2747.	2.2	32
386	Efficient removal of organic dye pollutants using covalent organic frameworks. AICHE Journal, 2017, 63, 3470-3478.	1.8	136
387	Persistent Electrochemical Performance in Epitaxial VO <sub>2</sub> (B). Nano Letters, 2017, 17, 2229-2233.	4.5	41
388	Quantitative and Atomic-Scale View of CO-Induced Pt Nanoparticle Surface Reconstruction at Saturation Coverage via DFT Calculations Coupled with <i>in Situ</i> TEM and IR. Journal of the American Chemical Society, 2017, 139, 4551-4558.	6.6	186
389	A sodium–aluminum hybrid battery. Journal of Materials Chemistry A, 2017, 5, 6589-6596.	5.2	25
390	Frontispiece: Mesoporous Carbon Materials with Functional Compositions. Chemistry - A European Journal, 2017, 23, .	1.7	2
391	High-Surface Area Ceria-Zirconia Films Prepared by Atomic Layer Deposition. Catalysis Letters, 2017, 147, 1464-1470.	1.4	13
392	Toward the Design of a Hierarchical Perovskite Support: Ultra-Sintering-Resistant Gold Nanocatalysts for CO Oxidation. ACS Catalysis, 2017, 7, 3388-3393.	5.5	40
393	Stiffness Evolution in Frozen Sands Subjected to Stress Changes. Journal of Geotechnical and Geoenvironmental Engineering - ASCE, 2017, 143, .	1.5	11
394	New Polymer Colloidal and Carbon Nanospheres: Stabilizing Ultrasmall Metal Nanoparticles for Solvent-Free Catalysis. Chemistry of Materials, 2017, 29, 4044-4051.	3.2	35
395	Solventâ€Free Selfâ€Assembly to the Synthesis of Nitrogenâ€Doped Ordered Mesoporous Polymers for Highly Selective Capture and Conversion of CO <sub>2</sub> . Advanced Materials, 2017, 29, 1700445.	11.1	162
396	Controlling the Intermediate Structure of an Ionic Liquid for f-Block Element Separations. Journal of Physical Chemistry Letters, 2017, 8, 2049-2054.	2.1	8

#	Article	IF	CITATIONS
397	In Situ Atomic-Scale Observation of the Two-Dimensional Co(OH) <sub>2</sub> Transition at Atmospheric Pressure. Chemistry of Materials, 2017, 29, 4572-4579.	3.2	26
398	Highly Efficient Carbon Monoxide Capture by Carbanionâ€Functionalized Ionic Liquids through Câ€Site Interactions. Angewandte Chemie, 2017, 129, 6947-6951.	1.6	26
399	Rücktitelbild: Highly Efficient Carbon Monoxide Capture by Carbanionâ€Functionalized Ionic Liquids through Câ€Site Interactions (Angew. Chem. 24/2017). Angewandte Chemie, 2017, 129, 7108-7108.	1.6	0
400	Highly Efficient Carbon Monoxide Capture by Carbanionâ€Functionalized Ionic Liquids through Câ€Site Interactions. Angewandte Chemie - International Edition, 2017, 56, 6843-6847.	7.2	83
401	Pdâ€Metalated Conjugated Nanoporous Polycarbazoles for Additiveâ€Free Cyanation of Aryl Halides: Boosting Catalytic Efficiency through Spatial Modulation. ChemSusChem, 2017, 10, 2320-2320.	3.6	0
402	Superacid-promoted synthesis of highly porous hypercrosslinked polycarbazoles for efficient CO <sub>2</sub> capture. Chemical Communications, 2017, 53, 7645-7648.	2.2	32
403	Uniform Pt/Pd Bimetallic Nanocrystals Demonstrate Platinum Effect on Palladium Methane Combustion Activity and Stability. ACS Catalysis, 2017, 7, 4372-4380.	5.5	124
404	Impact of gate geometry on ionic liquid gated ionotronic systems. APL Materials, 2017, 5, .	2.2	11
405	Promotion of Electrocatalytic Hydrogen Evolution Reaction on Nitrogen-Doped Carbon Nanosheets with Secondary Heteroatoms. ACS Nano, 2017, 11, 7293-7300.	7.3	357
406	Electrochemical Graphitization: An Efficient Conversion of Amorphous Carbons to Nanostructured Graphites. Chemistry - A European Journal, 2017, 23, 11455-11459.	1.7	52
407	Crystal Structural Effect of AuCu Alloy Nanoparticles on Catalytic CO Oxidation. Journal of the American Chemical Society, 2017, 139, 8846-8854.	6.6	181
408	Controlling interfacial properties in supported metal oxide catalysts through metal–organic framework templating. Journal of Materials Chemistry A, 2017, 5, 13565-13572.	5.2	15
409	Porous Structure Design of Polymeric Membranes for Gas Separation. Small Methods, 2017, 1, 1600051.	4.6	21
410	Pdâ€Metalated Conjugated Nanoporous Polycarbazoles for Additiveâ€Free Cyanation of Aryl Halides: Boosting Catalytic Efficiency through Spatial Modulation. ChemSusChem, 2017, 10, 2348-2351.	3.6	12
411	Design of Calix-Based Cages for CO <sub>2</sub> Capture. Industrial & Engineering Chemistry Research, 2017, 56, 4502-4507.	1.8	7
412	Surfactantâ€Assisted Stabilization of Au Colloids on Solids for Heterogeneous Catalysis. Angewandte Chemie, 2017, 129, 4565-4569.	1.6	18
413	Surfactantâ€Assisted Stabilization of Au Colloids on Solids for Heterogeneous Catalysis. Angewandte Chemie - International Edition, 2017, 56, 4494-4498.	7.2	129
414	Polydopamineâ€Inspired, Dual Heteroatomâ€Doped Carbon Nanotubes for Highly Efficient Overall Water Splitting. Advanced Energy Materials, 2017, 7, 1602068.	10.2	319

#	Article	IF	CITATIONS
415	Nitrogenâ€Doped CN <i><sub>x</sub></i> /CNTs Heteroelectrocatalysts for Highly Efficient Dyeâ€Sensitized Solar Cells. Advanced Energy Materials, 2017, 7, 1602276.	10.2	102
416	In Situ Coupling Strategy for the Preparation of FeCo Alloys and Co <sub>4</sub> N Hybrid for Highly Efficient Oxygen Evolution. Advanced Materials, 2017, 29, 1704091.	11.1	165
417	Sustainable synthesis of alkaline metal oxide-mesoporous carbons <i>via</i> mechanochemical coordination self-assembly. Journal of Materials Chemistry A, 2017, 5, 23446-23452.	5.2	22
418	Role of Electrical Double Layer Structure in Ionic Liquid Gated Devices. ACS Applied Materials & Interfaces, 2017, 9, 40949-40958.	4.0	24
419	Polythiophene coated aromatic polyimide enabled ultrafast and sustainable lithium ion batteries. Journal of Materials Chemistry A, 2017, 5, 24083-24090.	5.2	29
420	Tailoring Nâ€Terminated Defective Edges of Porous Boron Nitride for Enhanced Aerobic Catalysis. Small, 2017, 13, 1701857.	5.2	60
421	A general synthesis of abundant metal nanoparticles functionalized mesoporous graphitized carbon. RSC Advances, 2017, 7, 50966-50972.	1.7	6
422	Electrostaticâ€Assisted Liquefaction of Porous Carbons. Angewandte Chemie - International Edition, 2017, 56, 14958-14962.	7.2	56
423	In situ Study of Dynamics of CuAu Alloy Nanoparticles on Oxide Supports. Microscopy and Microanalysis, 2017, 23, 954-955.	0.2	0
424	Electrostaticâ€Assisted Liquefaction of Porous Carbons. Angewandte Chemie, 2017, 129, 15154-15158.	1.6	32
425	Effect of Surface Structure of TiO <sub>2</sub> Nanoparticles on CO <sub>2</sub> Adsorption and SO <sub>2</sub> Resistance. ACS Sustainable Chemistry and Engineering, 2017, 5, 9295-9306.	3.2	49
426	Efficient Functionalization of Polyethylene Fibers for the Uranium Extraction from Seawater through Atom Transfer Radical Polymerization. Industrial & Engineering Chemistry Research, 2017, 56, 10826-10832.	1.8	36
427	Preorganization and Cooperation for Highly Efficient and Reversible Capture of Lowâ€Concentration CO <sub>2</sub> by Ionic Liquids. Angewandte Chemie - International Edition, 2017, 56, 13293-13297.	7.2	128
428	Optimal Size of a Cylindrical Pore for Post-Combustion CO <sub>2</sub> Capture. Journal of Physical Chemistry C, 2017, 121, 22025-22030.	1.5	9
429	Solid-State Synthesis of Conjugated Nanoporous Polycarbazoles. ACS Macro Letters, 2017, 6, 1056-1059.	2.3	42
430	Catalyst Architecture for Stable Single Atom Dispersion Enables Site-Specific Spectroscopic and Reactivity Measurements of CO Adsorbed to Pt Atoms, Oxidized Pt Clusters, and Metallic Pt Clusters on TiO <sub>2</sub> . Journal of the American Chemical Society, 2017, 139, 14150-14165.	6.6	525
431	Aqueous and Templateâ€Free Synthesis of Meso–Macroporous Polymers for Highly Selective Capture and Conversion of Carbon Dioxide. ChemSusChem, 2017, 10, 4144-4149.	3.6	30
432	Preorganization and Cooperation for Highly Efficient and Reversible Capture of Low oncentration CO <sub>2</sub> by Ionic Liquids. Angewandte Chemie, 2017, 129, 13478-13482.	1.6	12

#	Article	IF	CITATIONS
433	Moltenâ€NaNH <sub>2</sub> Densified Graphene with Inâ€Plane Nanopores and Nâ€Doping for Compact Capacitive Energy Storage. Advanced Energy Materials, 2017, 7, 1700766.	10.2	23
434	Incorporating Rich Mesoporosity into a Ceria-Based Catalyst via Mechanochemistry. Chemistry of Materials, 2017, 29, 7323-7329.	3.2	45
435	New Atomic-Scale Insight into Self-Regeneration of Pt-CaTiO <sub>3</sub> Catalysts: Incipient Redox-Induced Structures Revealed by a Small-Angle Tilting STEM Technique. Journal of Physical Chemistry C, 2017, 121, 17348-17353.	1.5	27
436	In situ atomic-scale observation of oxygen-driven core-shell formation in Pt3Co nanoparticles. Nature Communications, 2017, 8, 204.	5.8	102
437	Twoâ€Ðimensional Materials as Prospective Scaffolds for Mixedâ€Matrix Membraneâ€Based CO <sub>2</sub> Separation. ChemSusChem, 2017, 10, 3304-3316.	3.6	77
438	In-situ observation of Rh-CaTiO3 catalysts during reduction and oxidation treatments by transmission electron microscopy. Microscopy and Microanalysis, 2017, 23, 948-949.	0.2	0
439	Neutron vibrational spectroscopic studies of novel tire-derived carbon materials. Physical Chemistry Chemical Physics, 2017, 19, 22256-22262.	1.3	8
440	Transmission electron microscopy with atomic resolution under atmospheric pressures. MRS Communications, 2017, 7, 798-812.	0.8	24
441	Origin of the unusually strong and selective binding of vanadium by polyamidoximes in seawater. Nature Communications, 2017, 8, 1560.	5.8	110
442	Materials for the Recovery of Uranium from Seawater. Chemical Reviews, 2017, 117, 13935-14013.	23.0	639
443	Mechanochemical synthesis of porous organic materials. Journal of Materials Chemistry A, 2017, 5, 16118-16127.	5.2	79
444	Poly(alkyl methacrylate) Brush-Grafted Silica Nanoparticles as Oil Lubricant Additives: Effects of Alkyl Pendant Groups on Oil Dispersibility, Stability, and Lubrication Property. ACS Applied Materials & Interfaces, 2017, 9, 25038-25048.	4.0	70
445	Revealing Surface Elemental Composition and Dynamic Processes Involved in Facet-Dependent Oxidation of Pt <sub>3</sub> Co Nanoparticles via <i>in Situ</i> Transmission Electron Microscopy. Nano Letters, 2017, 17, 4683-4688.	4.5	71
446	Polyethylenimine modified silica nanoparticles enhance interfacial interactions and desalination performance of thin film nanocomposite membranes. Journal of Membrane Science, 2017, 541, 19-28.	4.1	55
447	Efficient Absorption of SO <sub>2</sub> by EmimCl-EG Deep Eutectic Solvents. ACS Sustainable Chemistry and Engineering, 2017, 5, 6382-6386.	3.2	92
448	Observing Framework Expansion of Ordered Mesoporous Hard Carbon Anodes with Ionic Liquid Electrolytes via in Situ Small-Angle Neutron Scattering. ACS Energy Letters, 2017, 2, 1698-1704.	8.8	16
449	Versatile PbS Quantum Dot Ligand Exchange Systems in the Presence of Pbâ€Thiolates. Small, 2017, 13, 1602956.	5.2	23
450	A Novel Electrolyte Salt Additive for Lithiumâ€lon Batteries with Voltages Greater than 4.7 V. Advanced Energy Materials, 2017, 7, 1601397.	10.2	103

#	Article	IF	CITATIONS
451	Microengineered 3D cellâ€laden thermoresponsive hydrogels for mimicking cell morphology and orientation in cartilage tissue engineering. Biotechnology and Bioengineering, 2017, 114, 217-231.	1.7	61
452	Cellâ€penetrating peptide–labelled smart polymers for enhanced gene delivery. Engineering in Life Sciences, 2017, 17, 193-203.	2.0	6
453	Understanding functionalized silica nanoparticles incorporation in thin film composite membranes: Interactions and desalination performance. Journal of Membrane Science, 2017, 521, 53-64.	4.1	58
454	Frontispiece: Electrochemical Graphitization: An Efficient Conversion of Amorphous Carbons to Nanostructured Graphites. Chemistry - A European Journal, 2017, 23, .	1.7	0
455	Transmission Electron Microscopy at Atmospheric Pressure. Microscopy and Microanalysis, 2016, 22, 726-727.	0.2	0
456	Poly( <i>N</i> â€isopropylacrylamide) hydrogel/chitosan scaffold hybrid for threeâ€dimensional stem cell culture and cartilage tissue engineering. Journal of Biomedical Materials Research - Part A, 2016, 104, 2764-2774.	2.1	52
457	Multiâ€Molar Absorption of CO <sub>2</sub> by the Activation of Carboxylate Groups in Amino Acid Ionic Liquids. Angewandte Chemie - International Edition, 2016, 55, 7166-7170.	7.2	264
458	Thickness―and Particleâ€Sizeâ€Dependent Electrochemical Reduction of Carbon Dioxide on Thin‣ayer Porous Silver Electrodes. ChemSusChem, 2016, 9, 428-432.	3.6	43
459	New Insights into CO2 Absorption Mechanisms with Amino-Acid Ionic Liquids. ChemSusChem, 2016, 9, 765-765.	3.6	0
460	Formation of industrial mixed culture biofilm in chlorophenol cultivated medium of microbial fuel cell. AIP Conference Proceedings, 2016, , .	0.3	1
461	Thermoresponsive Acidic Microgels as Functional Draw Agents for Forward Osmosis Desalination. Environmental Science & Technology, 2016, 50, 4221-4228.	4.6	41
462	An integrated statistic and systematic approach to study correlation of synthesis condition and desalination performance of thin film composite membranes. Desalination, 2016, 394, 138-147.	4.0	31
463	Smart surface-enhanced Raman scattering traceable drug delivery systems. Nanoscale, 2016, 8, 12803-12811.	2.8	17
464	Chemical impact of catholytes on Bacillus subtilis-catalysed microbial fuel cell performance for degrading 2,4-dichlorophenol. Chemical Engineering Journal, 2016, 301, 103-114.	6.6	34
465	Mechanistic insight into the nucleation and growth of oleic acid capped lead sulphide quantum dots. Physical Chemistry Chemical Physics, 2016, 18, 14055-14062.	1.3	20
466	One-step synthesis of nitrogen-doped graphene-like meso-macroporous carbons as highly efficient and selective adsorbents for CO <sub>2</sub> capture. Journal of Materials Chemistry A, 2016, 4, 14567-14571.	5.2	67
467	Use of steric encumbrance to develop conjugated nanoporous polymers for metal-free catalytic hydrogenation. Chemical Communications, 2016, 52, 11919-11922.	2.2	17
468	Multicellular Spheroids Formation and Recovery in Microfluidics-generated Thermoresponsive Microgel Droplets. Colloids and Interface Science Communications, 2016, 14, 4-7.	2.0	17

#	Article	IF	CITATIONS
469	Highly ordered ZnMnO <sub>3</sub> nanotube arrays from a "self-sacrificial―ZnO template as high-performance electrodes for lithium ion batteries. Journal of Materials Chemistry A, 2016, 4, 16318-16323.	5.2	36
470	Design and synthesis of micro–meso–macroporous polymers with versatile active sites and excellent activities in the production of biofuels and fine chemicals. Green Chemistry, 2016, 18, 6536-6544.	4.6	30
471	A mechanistic study on tumour spheroid formation in thermosensitive hydrogels: experiments and mathematical modelling. RSC Advances, 2016, 6, 73282-73291.	1.7	27
472	Rational Design of Bi Nanoparticles for Efficient Electrochemical CO <sub>2</sub> Reduction: The Elucidation of Size and Surface Condition Effects. ACS Catalysis, 2016, 6, 6255-6264.	5.5	212
473	A Robust Strategy for "Living―Growth of Lead Sulfide Quantum Dots. ChemNanoMat, 2016, 2, 49-53.	1.5	4
474	Realizing Selective and Aerobic Oxidation by Porous Transition-Metal-Salt@Ceria Catalyst. ChemistrySelect, 2016, 1, 1179-1183.	0.7	3
475	Thermoresponsive cationic copolymer microgels as high performance draw agents in forward osmosis desalination. Journal of Membrane Science, 2016, 518, 273-281.	4.1	25
476	Hollow mesoporous silica nanoparticles: A peculiar structure for thin film nanocomposite membranes. Journal of Membrane Science, 2016, 519, 1-10.	4.1	72
477	Experimental evaluation of calcein and alizarin red S for immersion marking of silver carp <i>Hypophthalmichthys molitrix</i> (Valenciennes, 1844). Journal of Applied Ichthyology, 2016, 32, 83-91.	0.3	11
478	<i>In Situ</i> Doping Strategy for the Preparation of Conjugated Triazine Frameworks Displaying Efficient CO <sub>2</sub> Capture Performance. Journal of the American Chemical Society, 2016, 138, 11497-11500.	6.6	200
479	Degradation of 2,4-Dichlorophenol by Bacillus Subtilis with Concurrent Electricity Generation in Microbial Fuel Cell. Procedia Engineering, 2016, 148, 370-377.	1.2	15
480	Ordered Mesoporous Polymers for Biomass Conversions and Crossâ€Coupling Reactions. ChemSusChem, 2016, 9, 2496-2504.	3.6	27
481	A Sacrificial Coating Strategy Toward Enhancement of Metal–Support Interaction for Ultrastable Au Nanocatalysts. Journal of the American Chemical Society, 2016, 138, 16130-16139.	6.6	217
482	Solvothermal synthesis of hierarchically nanoporous organic polymers with tunable nitrogen functionality for highly selective capture of CO <sub>2</sub> . Journal of Materials Chemistry A, 2016, 4, 13063-13070.	5.2	78
483	Substitution Effect Guided Synthesis of Task-Specific Nanoporous Polycarbazoles with Enhanced Carbon Capture. Macromolecules, 2016, 49, 5325-5330.	2.2	38
484	Controlled Gas Exfoliation of Boron Nitride into Few‣ayered Nanosheets. Angewandte Chemie, 2016, 128, 10924-10928.	1.6	44
485	Boron Supercapacitors. ACS Energy Letters, 2016, 1, 1241-1246.	8.8	75
486	Hierarchically Superstructured Metal Sulfides: Facile Perturbationâ€Assisted Nanofusion Synthesis and Visible Light Photocatalytic Characterizations. ChemNanoMat, 2016, 2, 1104-1110.	1.5	8

#	Article	IF	CITATIONS
487	Generation of Fluorescent and Stable Conjugated Polymer Nanoparticles with Hydrophobically Modified Poly(acrylate)s. Macromolecules, 2016, 49, 8530-8539.	2.2	6
488	Hyper-crosslinked cyclodextrin porous polymer: an efficient CO <sub>2</sub> capturing material with tunable porosity. RSC Advances, 2016, 6, 110307-110311.	1.7	22
489	The water retention curve and relative permeability for gas production from hydrateâ€bearing sediments: poreâ€network model simulation. Geochemistry, Geophysics, Geosystems, 2016, 17, 3099-3110.	1.0	96
490	What can molecular simulation do for global warming?. Wiley Interdisciplinary Reviews: Computational Molecular Science, 2016, 6, 173-197.	6.2	32
491	Formation and development of salt crusts on soil surfaces. Acta Geotechnica, 2016, 11, 1103-1109.	2.9	46
492	TiN-coated micron-sized tantalum-doped Li4Ti5O12 with enhanced anodic performance for lithium-ion batteries. Journal of Alloys and Compounds, 2016, 687, 746-753.	2.8	39
493	Dynamical Observation and Detailed Description of Catalysts under Strong Metal–Support Interaction. Nano Letters, 2016, 16, 4528-4534.	4.5	230
494	Probing the interaction of ionic liquids with graphene using surfaceâ€enhanced Raman spectroscopy. Journal of Raman Spectroscopy, 2016, 47, 585-590.	1.2	18
495	Guestâ€Induced Breathing Effect in a Flexible Molecular Crystal. Angewandte Chemie, 2016, 128, 3439-3442.	1.6	4
496	Enhancement on the wettability of lithium battery separator toward nonaqueous electrolytes. Journal of Membrane Science, 2016, 503, 25-30.	4.1	95
497	Graphene oxide-polydopamine derived N, S-codoped carbon nanosheets as superior bifunctional electrocatalysts for oxygen reduction and evolution. Nano Energy, 2016, 19, 373-381.	8.2	597
498	Manipulation of nanofiber-based β-galactosidase nanoenvironment for enhancement of galacto-oligosaccharide production. Journal of Biotechnology, 2016, 222, 56-64.	1.9	30
499	Uranium Adsorbent Fibers Prepared by Atom-Transfer Radical Polymerization from Chlorinated Polypropylene and Polyethylene Trunk Fibers. Industrial & Engineering Chemistry Research, 2016, 55, 4130-4138.	1.8	46
500	Rational design and synthesis of a porous, task-specific polycarbazole for efficient CO <sub>2</sub> capture. Chemical Communications, 2016, 52, 4454-4457.	2.2	55
501	Recent advances in gold-metal oxide core-shell nanoparticles: Synthesis, characterization, and their application for heterogeneous catalysis. Frontiers of Chemical Science and Engineering, 2016, 10, 39-56.	2.3	38
502	Correlation of morphology with catalytic performance of CrO /Ce0.2Zr0.8O2 catalysts for NO oxidation via in-situ STEM. Chemical Engineering Journal, 2016, 288, 238-245.	6.6	21
503	Quantifying the binding strength of salicylaldoxime–uranyl complexes relative to competing salicylaldoxime–transition metal ion complexes in aqueous solution: a combined experimental and computational study. Dalton Transactions, 2016, 45, 9051-9064.	1.6	23
504	Synthesis of Naphthalimidedioxime Ligand-Containing Fibers for Uranium Adsorption from Seawater. Industrial & Engineering Chemistry Research, 2016, 55, 4161-4169.	1.8	40

#	Article	IF	CITATIONS
505	Self-supported electrocatalysts for advanced energy conversion processes. Materials Today, 2016, 19, 265-273.	8.3	268
506	Influence of polymer molecular weight on the in vitro cytotoxicity of poly (N-isopropylacrylamide). Materials Science and Engineering C, 2016, 59, 509-513.	3.8	30
507	Rücktitelbild: Hypercrosslinked Phenolic Polymers with Well-Developed Mesoporous Frameworks (Angew. Chem. 15/2015). Angewandte Chemie, 2015, 127, 4762-4762.	1.6	0
508	Synthesis of MCF-supported AuCo nanoparticle catalysts and the catalytic performance for the CO oxidation reaction. RSC Advances, 2015, 5, 100212-100222.	1.7	10
509	Elastic Properties of GaN Nanowires: Revealing the influence of planar defects on Young's modulus at nanoscale. Microscopy and Microanalysis, 2015, 21, 1915-1916.	0.2	42
510	Singleâ€cell analysis for bioprocessing. Engineering in Life Sciences, 2015, 15, 582-592.	2.0	5
511	Lowâ€Temperature CO Oxidation over a Ternary Oxide Catalyst with High Resistance to Hydrocarbon Inhibition. Angewandte Chemie, 2015, 127, 13461-13465.	1.6	8
512	Polycationâ€mediated gene delivery: Challenges and considerations for the process of plasmid DNA transfection. Engineering in Life Sciences, 2015, 15, 489-498.	2.0	34
513	Clinicopathological and phenotypic features of chronic <scp>NK</scp> cell lymphocytosis identified among patients with asymptomatic lymphocytosis. International Journal of Laboratory Hematology, 2015, 37, 783-790.	0.7	4
514	Porous Carbon Supports: Recent Advances with Various Morphologies and Compositions. ChemCatChem, 2015, 7, 2788-2805.	1.8	83
515	Frontispiece: Charged Porous Polymers using a Solid CO Cross-Coupling Reaction. Chemistry - A European Journal, 2015, 21, n/a-n/a.	1.7	0
516	Lowâ€Temperature CO Oxidation over a Ternary Oxide Catalyst with High Resistance to Hydrocarbon Inhibition. Angewandte Chemie - International Edition, 2015, 54, 13263-13267.	7.2	87
517	Innenrücktitelbild: Porous Liquids: A Promising Class of Media for Gas Separation (Angew. Chem.) Tj ETQq1 1 (	0.784314 1.6	rgBT /Overlo
518	Role of precursor chemistry in the direct fluorination to form titanium based conversion anodes for lithium ion batteries. RSC Advances, 2015, 5, 88876-88885.	1.7	14
519	γâ€PGA oated Mesoporous Silica Nanoparticles with Covalently Attached Prodrugs for Enhanced Cellular Uptake and Intracellular GSHâ€Responsive Release. Advanced Healthcare Materials, 2015, 4, 771-781.	3.9	54
520	Polydopamine–graphene oxide derived mesoporous carbon nanosheets for enhanced oxygen reduction. Nanoscale, 2015, 7, 12598-12605.	2.8	104
521	Stability and Core-Level Signature of Nitrogen Dopants in Carbonaceous Materials. Chemistry of Materials, 2015, 27, 5775-5781.	3.2	41
522	Constructing Hierarchical Interfaces: TiO <sub>2</sub> -Supported PtFe–FeO <sub><i>x</i></sub> Nanowires for Room Temperature CO Oxidation. Journal of the American Chemical Society, 2015, 137, 10156-10159.	6.6	86

#	Article	IF	CITATIONS
523	Hybridising nitrogen doped titania with kaolinite: A feasible catalyst for a semi-continuous photo-degradation reactor system. Chemical Engineering Journal, 2015, 279, 939-947.	6.6	8
524	Water desalination using nanoporous single-layer graphene. Nature Nanotechnology, 2015, 10, 459-464.	15.6	1,372
525	Confining Noble Metal (Pd, Au, Pt) Nanoparticles in Surfactant Ionic Liquids: Active Non-Mercury Catalysts for Hydrochlorination of Acetylene. ACS Catalysis, 2015, 5, 6724-6731.	5.5	94
526	An efficient low-temperature route to nitrogen-doping and activation of mesoporous carbons for CO <sub>2</sub> capture. Chemical Communications, 2015, 51, 17261-17264.	2.2	47
527	Hierarchical Mesoporous/Macroporous Perovskite La <sub>0.5</sub> Sr <sub>0.5</sub> CoO <sub>3–<i>x</i></sub> Nanotubes: A Bifunctional Catalyst with Enhanced Activity and Cycle Stability for Rechargeable Lithium Oxygen Batteries. ACS Applied Materials &: Interfaces. 2015. 7. 22478-22486.	4.0	130
528	Theoretical study of the coordination behavior of formate and formamidoximate with dioxovanadium( <scp>v</scp> ) cation: implications for selectivity towards uranyl. Physical Chemistry Chemical Physics, 2015, 17, 31715-31726.	1.3	27
529	Nanoprecipitation and Spectroscopic Characterization of Curcumin-Encapsulated Polyester Nanoparticles. Langmuir, 2015, 31, 11419-11427.	1.6	25
530	Sigmoid Correlations for Gas Solubility and Enthalpy Change of Chemical Absorption of CO <sub>2</sub> . Industrial & Engineering Chemistry Research, 2015, 54, 10126-10133.	1.8	29
531	Probing the Role of Zr Addition versus Textural Properties in Enhancement of CO <sub>2</sub> Adsorption Performance in Silica/PEI Composite Sorbents. Langmuir, 2015, 31, 9356-9365.	1.6	26
532	Surface Structure Dependence of SO <sub>2</sub> Interaction with Ceria Nanocrystals with Well-Defined Surface Facets. Journal of Physical Chemistry C, 2015, 119, 28895-28905.	1.5	26
533	Phosphorusâ€Doped Graphitic Carbon Nitrides Grown Inâ€Situ on Carbonâ€Fiber Paper: Flexible and Reversible Oxygen Electrodes. Angewandte Chemie - International Edition, 2015, 54, 4646-4650.	7.2	722
534	Functionalized thermo-responsive microgels for high performance forward osmosis desalination. Water Research, 2015, 70, 385-393.	5.3	62
535	Elastic Properties of GaN Nanowires: Revealing the Influence of Planar Defects on Young's Modulus at Nanoscale. Nano Letters, 2015, 15, 8-15.	4.5	60
536	Activating natural bentonite as a cost-effective adsorbent for removal of Congo-red in wastewater. Journal of Industrial and Engineering Chemistry, 2015, 21, 653-661.	2.9	133
537	Fabricating polystyrene fiber-dehydrogenase assemble as a functional biocatalyst. Enzyme and Microbial Technology, 2015, 68, 15-22.	1.6	18
538	Intracellular Microenvironmentâ€Responsive Dendrimerâ€Like Mesoporous Nanohybrids for Traceable, Effective, and Safe Gene Delivery. Advanced Functional Materials, 2014, 24, 7627-7637.	7.8	59
539	A biodegradable thermosensitive hydrogel with tuneable properties for mimicking three-dimensional microenvironments of stem cells. RSC Advances, 2014, 4, 63951-63961.	1.7	43
540	Synthesis and Characterization of Lithium Bis(fluoromalonato)borate for Lithiumâ€lon Battery Applications. Advanced Energy Materials, 2014, 4, 1301368.	10.2	43

#	Article	IF	CITATIONS
541	Easy synthesis of poly(ionic liquid) for use as a porous carbon precursor. New Carbon Materials, 2014, 29, 78-80.	2.9	7
542	Label-free dendrimer-like silica nanohybrids for traceable and controlled gene delivery. Biomaterials, 2014, 35, 5580-5590.	5.7	62
543	Mesoporous MnCo <sub>2</sub> O <sub>4</sub> with abundant oxygen vacancy defects as high-performance oxygen reduction catalysts. Journal of Materials Chemistry A, 2014, 2, 8676-8682.	5.2	227
544	Shape Control of Mn <sub>3</sub> O <sub>4</sub> Nanoparticles on Nitrogenâ€Doped Graphene for Enhanced Oxygen Reduction Activity. Advanced Functional Materials, 2014, 24, 2072-2078.	7.8	283
545	Endosomal pH responsive polymers for efficient cancer targeted gene therapy. Colloids and Surfaces B: Biointerfaces, 2014, 119, 55-65.	2.5	26
546	Intracellular Microenvironment Responsive Polymers: A Multipleâ€stage Transport Platform for Highâ€Performance Gene Delivery. Small, 2014, 10, 871-877.	5.2	21
547	Origin of Active Oxygen in a Ternary CuO <sub><i>x</i></sub> /Co <sub>3</sub> O <sub>4</sub> –CeO <sub>2</sub> Catalyst for CO Oxidation. Journal of Physical Chemistry C, 2014, 118, 27870-27877.	1.5	50
548	A non-micellar synthesis of mesoporous carbon via spinodal decomposition. RSC Advances, 2014, 4, 23703-23706.	1.7	4
549	A thermally responsive cationic nanogel-based platform for three-dimensional cell culture and recovery. RSC Advances, 2014, 4, 29146.	1.7	25
550	Intracellular Microenvironmentâ€Responsive Labelâ€Free Autofluorescent Nanogels for Traceable Gene Delivery. Advanced Healthcare Materials, 2014, 3, 1839-1848.	3.9	28
551	Synthesis of Highly Active and Stable Spinelâ€Type Oxygen Evolution Electrocatalysts by a Rapid Inorganic Selfâ€Templating Method. Chemistry - A European Journal, 2014, 20, 12669-12676.	1.7	42
552	Interactions of Organic Solvents at Graphene/α-Al <sub>2</sub> O <sub>3</sub> and Graphene Oxide/α-Al <sub>2</sub> O <sub>3</sub> Interfaces Studied by Sum Frequency Generation. Journal of Physical Chemistry C, 2014, 118, 17745-17755.	1.5	13
553	Synthesis and Acid Solution Properties of Two-head Group Viscoelastic Surfactant. Petroleum Science and Technology, 2014, 32, 729-737.	0.7	2
554	Molecular Dynamics Simulation of Anion Effect on Solubility, Diffusivity, and Permeability of Carbon Dioxide in Ionic Liquids. Industrial & Engineering Chemistry Research, 2014, 53, 10485-10490.	1.8	48
555	Metal–Organic Framework Derived Hybrid Co <sub>3</sub> O <sub>4</sub> -Carbon Porous Nanowire Arrays as Reversible Oxygen Evolution Electrodes. Journal of the American Chemical Society, 2014, 136, 13925-13931.	6.6	1,744
556	Protonâ€Functionalized Twoâ€Đimensional Graphitic Carbon Nitride Nanosheet: An Excellent Metalâ€∤Labelâ€Free Biosensing Platform. Small, 2014, 10, 2382-2389.	5.2	441
557	Mechanical properties of pH-responsive poly(2-hydroxyethyl methacrylate/methacrylic acid) microgels prepared by inverse microemulsion polymerization. Reactive and Functional Polymers, 2014, 74, 101-106.	2.0	14
558	Polymeric molecular sieve membranes via in situ cross-linking of non-porous polymer membrane templates. Nature Communications, 2014, 5, 3705.	5.8	143

#	Article	IF	CITATIONS
559	Strainâ€Based In Situ Study of Anion and Cation Insertion into Porous Carbon Electrodes with Different Pore Sizes. Advanced Energy Materials, 2014, 4, 1300683.	10.2	39
560	Graphitic Carbon Nitride Nanosheet–Carbon Nanotube Threeâ€Dimensional Porous Composites as Highâ€Performance Oxygen Evolution Electrocatalysts. Angewandte Chemie - International Edition, 2014, 53, 7281-7285.	7.2	737
561	Amphiphilic and biocompatible properties of poly (EAâ€MAA). Journal of Applied Polymer Science, 2013, 127, 3731-3736.	1.3	1
562	Efficient CO <sub>2</sub> Capture by a 3D Porous Polymer Derived from Tröger's Base. ACS Macro Letters, 2013, 2, 660-663.	2.3	138
563	The strategies for improving carbon dioxide chemisorption by functionalized ionic liquids. RSC Advances, 2013, 3, 15518.	1.7	127
564	Developing Functionalized Dendrimerâ€Like Silica Nanoparticles with Hierarchical Pores as Advanced Delivery Nanocarriers. Advanced Materials, 2013, 25, 5981-5985.	11.1	199
565	Formation of Iron Oxyfluoride Phase on the Surface of Nano-Fe3O4 Conversion Compound for Electrochemical Energy Storage. Journal of Physical Chemistry Letters, 2013, 4, 3798-3805.	2.1	28
566	Deposition–Precipitation and Stabilization of a Silica-Supported Au Catalyst by Surface Modification with Carbon Nitride. Catalysis Letters, 2013, 143, 1339-1345.	1.4	11
567	Developing a chitosan supported imidazole Schiff-base for high-efficiency gene delivery. Polymer Chemistry, 2013, 4, 840-850.	1.9	49
568	Nitrogenâ€Enriched Carbons from Alkali Salts with High Coulombic Efficiency for Energy Storage Applications. Advanced Energy Materials, 2013, 3, 708-712.	10.2	51
569	Towards the selective modification of soft-templated mesoporous carbon materials by elemental fluorine for energy storage devices. Journal of Materials Chemistry A, 2013, 1, 9327.	5.2	22
570	Distinctive Nanoscale Organization of Dicationic versus Monocationic Ionic Liquids. Journal of Physical Chemistry C, 2013, 117, 18251-18257.	1.5	66
571	Water retention curve for hydrateâ€bearing sediments. Geophysical Research Letters, 2013, 40, 5637-5641.	1.5	39
572	Carbon Membranes: New Tricks for Old Molecules: Development and Application of Porous Nâ€doped, Carbonaceous Membranes for CO <sub>2</sub> Separation (Adv. Mater. 30/2013). Advanced Materials, 2013, 25, 4200-4200.	11.1	0
573	Hydrate morphology: Physical properties of sands with patchy hydrate saturation. Journal of Geophysical Research, 2012, 117, .	3.3	231
574	Windowed Carbon Nanotubes for Efficient CO <sub>2</sub> Removal from Natural Gas. Journal of Physical Chemistry Letters, 2012, 3, 3343-3347.	2.1	68
575	Nitrogen-Doped Mesoporous Carbon for Carbon Capture – A Molecular Simulation Study. Journal of Physical Chemistry C, 2012, 116, 7106-7110.	1.5	48
576	Exploring thermal reversible hydrogels for stem cell expansion in three-dimensions. Soft Matter, 2012, 8, 7250.	1.2	31

#	Article	IF	CITATIONS
577	Polymer Microbead-Based Surface Enhanced Raman Scattering Immunoassays. Journal of Physical Chemistry C, 2012, 116, 17174-17181.	1.5	18
578	Electron-Beam-Induced Elastic–Plastic Transition in Si Nanowires. Nano Letters, 2012, 12, 2379-2385.	4.5	63
579	Structures and Energetics of Pt Clusters on TiO <sub>2</sub> : Interplay between Metal–Metal Bonds and Metal–Oxygen Bonds. Journal of Physical Chemistry C, 2012, 116, 21880-21885.	1.5	39
580	Silica-Supported Au–CuO <sub><i>x</i></sub> Hybrid Nanocrystals as Active and Selective Catalysts for the Formation of Acetaldehyde from the Oxidation of Ethanol. ACS Catalysis, 2012, 2, 2537-2546.	5.5	105
581	Ionic Liquid and Silica Sol-Gel Composite Materials Doped with N,N,N′,N′-tetra( <i>n</i> -octyl)diglycolamide for Extraction of La <sup>3+</sup> and Ba <sup>2+</sup> . Separation Science and Technology, 2012, 47, 244-249.	1.3	14
582	Exploring low-positively charged thermosensitive copolymers as gene delivery vectors. Soft Matter, 2012, 8, 1385-1394.	1.2	25
583	Exploring <i>N</i> -Imidazolyl- <i>O</i> -Carboxymethyl Chitosan for High Performance Gene Delivery. Biomacromolecules, 2012, 13, 146-153.	2.6	74
584	The enhancement of neural stem cell survival and growth by coculturing with expanded sertoli cells in vitro. Biotechnology Progress, 2012, 28, 196-205.	1.3	9
585	Synthesis of silica supported AuCu nanoparticle catalysts and the effects of pretreatment conditions for the CO oxidation reaction. Physical Chemistry Chemical Physics, 2011, 13, 2571.	1.3	92
586	Quantifying the defect-dominated size effect of fracture strain in single crystalline ZnO nanowires. Journal of Applied Physics, 2011, 109, 123504.	1.1	17
587	Low-Temperature Fluorination of Soft-Templated Mesoporous Carbons for a High-Power Lithium/Carbon Fluoride Battery. Chemistry of Materials, 2011, 23, 4420-4427.	3.2	102
588	A galactosamine-mediated drug delivery carrier for targeted liver cancer therapy. Pharmacological Research, 2011, 64, 410-419.	3.1	73
589	Interaction of Gold Clusters with a Hydroxylated Surface. Journal of Physical Chemistry Letters, 2011, 2, 1211-1215.	2.1	39
590	Benzyl-Functionalized Room Temperature Ionic Liquids for CO <sub>2</sub> /N <sub>2</sub> Separation. Industrial & Engineering Chemistry Research, 2011, 50, 14061-14069.	1.8	61
591	Sustainable development and energy geotechnology — Potential roles for geotechnical engineering. KSCE Journal of Civil Engineering, 2011, 15, 611-621.	0.9	41
592	"Brickâ€andâ€Mortar―Selfâ€Assembly Approach to Graphitic Mesoporous Carbon Nanocomposites. Advanced Functional Materials, 2011, 21, 2208-2215.	7.8	98
593	Coincorporation of nanoâ€silica and nanoâ€calcium carbonate in polypropylene. Journal of Applied Polymer Science, 2011, 121, 3007-3013.	1.3	9
594	Frabicating hydroxyapatite nanorods using a biomacromolecule template. Applied Surface Science, 2011, 257, 3174-3179.	3.1	31

#	Article	IF	CITATIONS
595	ABC block copolymer as "smart―pH-responsive carrier for intracellular delivery of hydrophobic drugs. Polymer, 2011, 52, 3396-3404.	1.8	34
596	Biomimetic three-dimensional microenvironment for controlling stem cell fate. Interface Focus, 2011, 1, 792-803.	1.5	60
597	Spherical N-carboxyethylchitosan/hydroxyapatite nanoparticles prepared by ionic diffusion process in a controlled manner. Journal of Materials Science: Materials in Medicine, 2010, 21, 3095-3101.	1.7	8
598	Self-assembly of N-maleoylchitosan in aqueous media. Colloids and Surfaces B: Biointerfaces, 2010, 76, 221-225.	2.5	16
599	Synthesis and properties of polystyreneâ€ <i>g</i> â€mSiO <sub>2</sub> filled polypropylene nanocomposites. Polymer Composites, 2010, 31, 807-815.	2.3	9
600	Atomic Structure of Au Nanoparticles on a Silica Support by an X-ray PDF Study. Journal of Physical Chemistry C, 2010, 114, 6983-6988.	1.5	7
601	Metal-containing polystyrene beads as standards for mass cytometry. Journal of Analytical Atomic Spectrometry, 2010, 25, 260.	1.6	43
602	Polysaccharide surface modified Fe3O4 nanoparticles for camptothecin loading and release. Acta Biomaterialia, 2009, 5, 1489-1498.	4.1	84
603	Synthesis of sulfur-containing aryl and heteroaryl vinyls via Suzuki–Miyaura cross-coupling for the preparation of SERS-active polymers. Tetrahedron Letters, 2009, 50, 5467-5469.	0.7	13
604	Thermo- and photo-responsive polymeric systems. Soft Matter, 2009, , .	1.2	39
605	Lanthanide-Containing Polymer Microspheres by Multiple-Stage Dispersion Polymerization for Highly Multiplexed Bioassays. Journal of the American Chemical Society, 2009, 131, 15276-15283.	6.6	92
606	Synthesis and Physicochemical Properties of Biocompatible N-carboxyethylchitosan. Journal of Biomaterials Science, Polymer Edition, 2009, 20, 981-992.	1.9	12
607	Preparation of N-Maleoylchitosan Nanocapsules for Loading and Sustained Release of Felodipine. Biomacromolecules, 2009, 10, 1997-2002.	2.6	14
608	Influence of anionic surfactant on the rheological properties of hydrophobically modified polyethylene-oxide/cyclodextrin inclusion complexes. Journal of Rheology, 2009, 53, 293-308.	1.3	8
609	Not All Anionic Polyelectrolytes Complex with DTAB. Langmuir, 2009, 25, 13712-13717.	1.6	16
610	Chitosan-poly(acrylic acid) complex modified paramagnetic Fe3O4 nanoparticles for camptothecin loading and release. Journal of Materials Research, 2009, 24, 2307-2315.	1.2	15
611	A facile synthesis of monodisperse Au nanoparticles and their catalysis of CO oxidation. Nano Research, 2008, 1, 229-234.	5.8	398
612	Polypyrrole-Based Nitrogen-Doped Carbon Replicas of SBA-15 and SBA-16 Containing Magnetic Nanoparticles. Journal of Physical Chemistry C, 2008, 112, 13126-13133.	1.5	66

#	Article	lF	CITATIONS
613	Preparation of Well-Dispersed Superparamagnetic Iron Oxide Nanoparticles in Aqueous Solution with Biocompatible <i>N</i> -Succinyl- <i>O</i> -carboxymethylchitosan. Journal of Physical Chemistry C, 2008, 112, 5432-5438.	1.5	52
614	pH-Responsive polymers: synthesis, properties and applications. Soft Matter, 2008, 4, 435.	1.2	593
615	Nano-fractals from inorganic salts induced by fullerene polymer systems. International Journal of Nanotechnology, 2007, 4, 377.	0.1	0
616	Rheological Properties of a Telechelic Associative Polymer in the Presence of α- and Methylated β-Cyclodextrins. Journal of Physical Chemistry B, 2007, 111, 371-378.	1.2	8
617	Interaction between Fluorocarbon End-Capped Poly(ethylene oxide) and Cyclodextrins. Macromolecules, 2007, 40, 2936-2945.	2.2	14
618	Fullerene Containing Polymers: A Review on Their Synthesis and Supramolecular Behavior in Solution. Journal of Nanoscience and Nanotechnology, 2007, 7, 1176-1196.	0.9	45
619	Effect of Cosolvents on the Binding Interaction between Poly(ethylene oxide) and Sodium Dodecyl Sulfate. Journal of Physical Chemistry B, 2006, 110, 20794-20800.	1.2	26
620	Self-Assembly of Well-Defined Mono and Dual End-Capped C60Containing Polyacrylic Acids in Aqueous Solution. Langmuir, 2006, 22, 7167-7174.	1.6	31
621	Isothermal titration calorimetric studies on the interaction between sodium dodecyl sulfate and polyethylene glycols of different molecular weights and chain architectures. Colloids and Surfaces A: Physicochemical and Engineering Aspects, 2006, 289, 200-206.	2.3	19
622	Salt effects on aggregation of O-carboxymethylchitosan in aqueous solution. Colloids and Surfaces B: Biointerfaces, 2006, 47, 20-28.	2.5	24
623	Laser light scattering and isothermal titration calorimetric studies of poly(ethylene oxide) aqueous solution in presence of sodium dodecyl sulfate. Journal of Colloid and Interface Science, 2005, 292, 79-85.	5.0	24
624	Self-assembly of C60 containing poly(methyl methacrylate) in ethyl acetate/decalin mixtures solvent. Polymer, 2005, 46, 4714-4721.	1.8	28
625	The aggregation behavior of O-carboxymethylchitosan in dilute aqueous solution. Colloids and Surfaces B: Biointerfaces, 2005, 43, 143-149.	2.5	119
626	Self-Assembly of Stimuli-Responsive Water-Soluble [60]Fullerene End-Capped Ampholytic Block Copolymer. Journal of Physical Chemistry B, 2005, 109, 4431-4438.	1.2	51
627	Dynamic light scattering of semidilute hydrophobically modified alkali-soluble emulsion solutions with different lengths of poly(ethylene oxide) spacer chain. Journal of Polymer Science, Part B: Polymer Physics, 2005, 43, 3288-3298.	2.4	7
628	Microstructure of Un-neutralized Hydrophobically Modified Alkali-Soluble Emulsion Latex in Different Surfactant Solutions. Langmuir, 2005, 21, 7136-7142.	1.6	6
629	Synthesis and Self-Assembly of [60]Fullerene Containing Sulfobetaine Polymer in Aqueous Solution. Journal of Physical Chemistry B, 2005, 109, 22791-22798.	1.2	31
630	Self-Assembly of Alkali-Soluble [60]Fullerene Containing Poly(methacrylic acid) in Aqueous Solution. Macromolecules, 2005, 38, 933-939.	2.2	55

#	Article	IF	CITATIONS
631	Rheological properties of hydrophobic ethoxylated urethane (HEUR) in the presence of methylated β-cyclodextrin. Polymer, 2004, 45, 8339-8348.	1.8	24
632	Formation of Oriented Nanostructures from Single Molecules of Conjugated Polymers in Microdroplets of Solution:Â The Role of Solvent. Macromolecules, 2004, 37, 6132-6140.	2.2	32
633	Self-Assembly Behavior of a Stimuli-Responsive Water-Soluble [60]Fullerene-Containing Polymer. Langmuir, 2004, 20, 8569-8575.	1.6	57
634	Solvent-Induced Large Compound Vesicle of [60]Fullerene Containing Poly(tert-butyl methacrylate). Langmuir, 2004, 20, 9882-9884.	1.6	31
635	Isothermal Titration Calorimetric Studies on the Temperature Dependence of Binding Interactions between Poly(propylene glycol)s and Sodium Dodecyl Sulfate. Langmuir, 2004, 20, 2177-2183.	1.6	101
636	Synthesis and Aggregation Behavior of Amphiphilic Block Copolymers in Aqueous Solution:Â Di- and Triblock Copolymers of Poly(ethylene oxide) and Poly(ethyl acrylate). Langmuir, 2004, 20, 1597-1604.	1.6	40
637	Isothermal Titration Calorimetric and Electromotive Force Studies on Binding Interactions of Hydrophobic Ethoxylated Urethane and Sodium Dodecyl Sulfate of Different Molecular Masses. Journal of Physical Chemistry B, 2004, 108, 4979-4988.	1.2	30
638	Polymer-Induced Fractal Patterns of [60]Fullerene Containing Poly(methacrylic acid) in Salt Solutions. Langmuir, 2004, 20, 9901-9904.	1.6	29
639	Isothermal titration calorimetric studies of alkyl phenol ethoxylate surfactants in aqueous solutions. Colloids and Surfaces A: Physicochemical and Engineering Aspects, 2003, 229, 157-168.	2.3	54
640	Aggregation behavior of two-arm fullerene-containing poly(ethylene oxide). Polymer, 2003, 44, 2529-2536.	1.8	68
641	Aggregation Behavior of C60-End-Capped Poly(ethylene oxide)s. Langmuir, 2003, 19, 4798-4803.	1.6	97
642	Novel pH-Responsive Amphiphilic Diblock Copolymers with Reversible Micellization Properties. Langmuir, 2003, 19, 5175-5177.	1.6	100
643	Rheology and Aggregation Behavior of Hydrophobically Modified Urethane Ethoxylate in Ethylene Glycolâ <sup>~•</sup> Water Mixtures. Macromolecules, 2003, 36, 6260-6266.	2.2	12
644	Dynamic Light Scattering of Semi-Dilute Hydrophobically Modified Alkali-Soluble Emulsion Solutions with Varying Length of Hydrophobic Alkyl Chains. Macromolecular Chemistry and Physics, 2002, 203, 2312-2321.	1.1	19
645	Isothermal Titration Calorimetry Studies of Binding Interactions between Polyethylene Glycol and Ionic Surfactants. Journal of Physical Chemistry B, 2001, 105, 10759-10763.	1.2	134
646	Binding Characteristics of Hydrophobic Ethoxylated Urethane (HEUR) and an Anionic Surfactant:Â Microcalorimetry and Laser Light Scattering Studies. Journal of Physical Chemistry B, 2001, 105, 10189-10196.	1.2	43
647	Microstructure of Dilute Telechelic Associative Polymer in Sodium Dodecyl Sulfate Solutions. Macromolecules, 2001, 34, 4673-4675.	2.2	18
648	Isothermal Titration Calorimetric Studies on Interactions of Ionic Surfactant and Poly(oxypropylene)â^'Poly(oxyethylene)â^' Poly(oxypropylene) Triblock Copolymers in Aqueous Solutions. Macromolecules, 2001, 34, 7049-7055.	2.2	85

#	Article	IF	CITATIONS
649	Light Scattering of Hydrophobically Modified Alkali-Soluble Emulsion (HASE) Polymer: Ionic Strength and Temperature Effects. Macromolecular Chemistry and Physics, 2001, 202, 335-342.	1.1	22
650	Aggregation behavior of methacrylic acid/ethyl acrylate copolymer in dilute solutions. European Polymer Journal, 2000, 36, 2671-2677.	2.6	37
651	Funtionalized Solâ~'Gels for Selective Copper(II) Separation. Environmental Science & Technology, 2000, 34, 2209-2214.	4.6	55
652	Microstructure of Dilute Hydrophobically Modified Alkali Soluble Emulsion in Aqueous Salt Solution. Macromolecules, 2000, 33, 404-411.	2.2	56
653	Light Scattering of Dilute Hydrophobically Modified Alkali-Soluble Emulsion Solutions:Â Effects of Hydrophobicity and Spacer Length of Macromonomer. Macromolecules, 2000, 33, 7021-7028.	2.2	50
654	Molar Conductance of Sodium Bromide and Sodium Iodide in Methanol + Water at 298.15 K. Journal of Chemical & Engineering Data, 1997, 42, 651-654.	1.0	18
655	Comparative UVâ^'Vis Studies of Uranyl Chloride Complex in Two Basic Ambient-Temperature Melt Systems:  The Observation of Spectral and Thermodynamic Variations Induced via Hydrogen Bonding. Inorganic Chemistry, 1997, 36, 4900-4902.	1.9	79
656	19F NMR study of 1-halo-F-adamantanes. Magnetic Resonance in Chemistry, 1993, 31, 969-971.	1.1	1
657	Europium Oxychloride Absorption Spectroscopy as an Optical Probe of Temperature. Spectroscopy Letters, 1993, 26, 1073-1083.	0.5	2
658	Preparation of C70-Doped Solid Silica Gel via Sol-Gel Process. Journal of the American Ceramic Society, 1992, 75, 2865-2866.	1.9	39
659	Fluorination of MXene by Elemental F <sub>2</sub> as Electrode Material for Lithiumâ€lon Batteries. ChemSusChem, 0, , .	3.6	0
660	Operando Metalloid Znδ+ Active Sites for Highly Efficient Carbon Dioxide Reduction Electrocatalysis. Angewandte Chemie, 0, , .	1.6	0
661	Molecular Dynamics Simulations of U(III) and U(IV) in Molten Chlorides. ACS Symposium Series, 0, , 365-386.	0.5	1